SLAC Proposal E-130

Supplement No. 1

May 5, 1977

SLAC PROPOSAL - E130

Precise Measurements of Asymmetries in Deep Inelastic Scattering of Polarized Electrons by Polarized Protons and by Polarized Deuterons

Yale-SLAC-Bielefeld-Tsukuba Group
(V.W. Hughes, correspondent)
First submitted, December 23, 1976
Revised, May 2, 1977

Title: Precise measurements of asymmetries in deep inelastic scattering of polarized electrons by polarized protons and by polarized deuterons.

Experimenters: V.W. Hughes (correspondent), Yale University
M.J. Alguard, M.R. Bergstrom, J.E. Clendenin, S. Dhawan, R. Fong-Tom
V.W. Hughes, M.S. Lubell, R.F. Oppenheim, D.A. Palmer, N. Sasao, K.P
Schüler, P.A. Souder, and M.E. Zeller - Yale University.

R.H. Miller and S.J. St Lorant - SLAC.

G. Baum and W. Raith - University of Bielefeld, West Germany.

K. Kondo and S. Miyashita - University of Tsukuba, Japan.
K. Morimoto, KEK, Japan

Beam: Polarized electron (PEGGY I). Energy, 22 GeV; current, 1.5×10^9 e^-/pulse; pulse length, 1.5 μsec; pulse repetition rate, 180 pps.

Target: Hydrocarbon polarized proton or polarized deuteron target, 2.5 cm x 2.5 cm x 3.8 cm. Set up in End Station A (ESA).

Experimental equipment and materials requested of SLAC
- One deflector magnet, 5D36
- Beam monitors: Two toroid charge monitors (#0 and #1);
- Beam dump, SEQ, and associated shielding
- One spectrometer using two existing ESA magnets
  - Supporting frame for magnets and detector house
  - Substantial shielding for detector house
- Lead glass shower counter (available from SFG)
- Counting room electronics (ESA)
- Existing SLAC-Yale polarized target
  - Liquid He for polarized target (220 ℓ/day); also LN_2 (100 ℓ/day
- Möller spectrometer being developed for E122

Date when equipment ready:
- Polarized electron source (Fall, 1977).
- Polarized target (Spring, 1978).
- Spectrometer (Summer, 1978).

Running time required:
- Check out: 250 hrs at 10 to 30 pps.
- Data-taking: 600 hrs at 180 pps.

Computers and data analysis:
- One SDS 9300 in ESA counting house for program debugging-
- One SDS 9300 in ESA counting house for on-line data taking.
- SLAC 360-91 for off-line analysis - 100 hrs.
- Period required for data analysis - about 6 months.

Table of Contents

Abstract

Relatively precise measurements of asymmetries in deep inelastic scattering of polarized electrons by polarized protons and by polarized deuterons are proposed. More than an order of magnitude increase in data rate as compared to SLAC experiment E-80 will be achieved, principally by the use of a larger acceptance spectrometer. A wider kinematic range will be studied extending from about $\omega = 1.5$ to $\omega = 13$, with Q^2 values up to 9 $(GeV/c)^2$. These measurements should yield overall precisions in the determination of the virtual photon-proton asymmetry A_1^p of about 0.03 to 0.08, as compared to our present E80 errors of 0.1 to 0.25. From the deuteron and proton measurements the virtual photon-neutron asymmetry A_1^n should be determined with an error of about 0.05 to 0.10.

The much more precise data on A_1^p over a wider kinematic range, and in particular for lower ω and higher Q^2 values, will improve significantly the test of scaling for A_1^p and will provide unique information about the spin structure of the nucleon to distinguish and test models of proton structure. Data on the neutron asymmetry A_1^n (which will be more accurate than our E80 data on the proton) will be the first such information and hence is exploratory. It will provide a new test of the quark-parton viewpoint for the neutron, including the predictions of the models for the spin structure of the neutron and an improved test of the Bjorken sum rule which requires values of A_1^n.

I. Status of SLAC E-80 Results, Including 1976 On-Line Results.

Introduction.

Physical Review Letters (M.J. Alguard et al., Phys. Rev. Lett. 37, 1258 (1976); 37, 1261 (1976).

Graph indicating kinematic points measured in 1975 and 1976 (Figure 1)

Deep inelastic scattering.

Table 1 of asymmetry values.

Graph of A_1 values and comparison with some theories (Figure 2).

Bjorken sum rule (Figure 3).

Resonance region.

Table 2 of asymmetry values.

Graph of asymmetry values (Figure 4).

Introduction

During the three cycles of our data-taking period for SLAC E-80 we made asymmetry measurements for one elastic, seven (7) deep inelastic, and seven (7) resonance region points. Fig. 1 shows our data points as a function of ν and Q^2, where ν is the laboratory virtual photon energy and Q^2 is its four momentum squared. Our deep inelastic points covered the range of ω from 2 to 10 with Q^2 of 1.0 to 4.0 $(GeV/c)^2$.

Off-line analysis is completed for the data taken in 1975, and the results are published in Phys. Rev. Lett. 37, 1258 (1976); 37, 1261 (1976). (Our notation is defined in these publications.)

Table 1 and Table 2 show the published and the preliminary (on-line) results of the asymmetry measurements in the deep inelastic and resonance regions, respectively. Measured values for $A/D \approx A_1$ are plotted in Fig. 2, together with several theoretical predictions for A_1 in deep inelastic scattering. Fig. 3 shows the on-line resonance region data.

Off-line analysis of our 1976 elastic and deep inelastic data is well under way and we expect to have final asymmetry values within 1 or 2 months. The effect of radiative corrections is also being studied, and we expect to have useful answers this summer. For the lower ω deep inelastic points radiative corrections to the asymmetry values are expected to be small, but for the ω=10 point the correction is estimated to be significant.

We have evaluated the integral appearing in the Bjorken sum rule using our data together with the assumptions $A_2^p = 0$ and $A_1^n = 0$ (Fig. 3; p. 10).

Generally, our deep inelastic results, which give large positive values for the lepton-proton asymmetry A and hence also for the virtual photon-proton asymmetry A_1, confirm the predictions of the quark-parton viewpoint. The Bjorken sum rule, scaling for A_1, and the proton model predictions for A_1 are consistent with our results.

The studies in the resonance region were exploratory. Beyond the off-line determination of asymmetry values, considerable analysis will be required to account for radiative and background corrections. Then the implications of the results for duality predictions on the spin dependence of resonance electroproduction and their relation to results from multipole analysis of other photoproduction and electroproduction data must be considered.

VOLUME 37, NUMBER 19 PHYSICAL REVIEW LETTERS 8 NOVEMBER 1976

Elastic Scattering of Polarized Electrons by Polarized Protons*

M. J. Alguard, W. W. Ash, G. Baum, J. E. Clendenin, P. S. Cooper, D. H. Coward, R. D. Ehrlich, A. Etkin, V. W. Hughes, H. Kobayakawa, K. Kondo, M. S. Lubell, R. H. Miller, D. A. Palmer, W. Raith, N. Sasao, K. P. Schüler, D. J. Sherden, C. K. Sinclair, and P. A. Souder

University of Bielefeld, Bielefeld, West Germany, and City University of New York, New York, New York 10031, and Nagoya University, Nagoya, Japan, and Stanford Linear Accelerator Center, Stanford, California 94305, and University of Tsukuba, Ibaraki, Japan, and Yale University, New Haven, Connecticut 06520

(Received 5 August 1976)

We report on a new type of high-energy electron-proton scattering experiment in which longitudinally polarized electrons are scattered from longitudinally polarized protons. The asymmetry in elastic scattering at $Q^2 = 0.765$ (GeV/c)^2 was measured; our result agrees with the theoretical asymmetry and determines the sign of G_E/G_M to be positive.

In this Letter we describe a high-energy electron-proton scattering experiment in which polarized electrons are scattered from polarized protons, and present the first results for elastic scattering. Our first results for deep inelastic scattering are reported in the following Letter.[1]

The momentum and scattering angle of the scattered electrons were measured when longitudinally polarized electrons were scattered from longitudinally polarized protons. The basic quantity measured was the antiparallel-parallel asymmetry A in the differential cross sections given by

$$A = \frac{d\sigma(\uparrow\downarrow) - d\sigma(\uparrow\uparrow)}{d\sigma(\uparrow\downarrow) + d\sigma(\uparrow\uparrow)}, \tag{1}$$

in which $d\sigma$ denotes the differential cross section $d\sigma(E, \theta)/d\Omega$ for incident electron energy E and laboratory scattering angle θ, and the arrows denote the antiparallel and parallel spin configurations.

If elastic scattering is described by the one-photon-exchange approximation, then the asymmetry can be expressed as[2]

$$A = \frac{\tau G_M}{G_E}\left\{\frac{2M}{E} + \frac{G_M}{G_E}\left[\frac{2\tau M}{E} + 2(1+\tau)\tan^2\frac{\theta}{2}\right]\right\} \times \left\{1 + \tau\left(\frac{G_M}{G_E}\right)^2\left[1 + 2(1+\tau)\tan^2\frac{\theta}{2}\right]\right\}^{-1}, \tag{2}$$

in which $\tau = Q^2/4M^2$, $q^2 = -Q^2 = -4EE'\sin^2(\theta/2)$ is the square of the four-momentum of the virtual photon, M is the proton mass, E' is the scattered electron energy, and G_E and G_M are the electric and magnetic elastic form factors of the proton. The electron mass has been neglected. We chose to measure A for elastic scattering primarily to test the validity of our experimental method. Alternatively, we can regard our measurement as a test of Eq. (2) and as a determination of the sign of G_E/G_M.

The polarized electron source (PEGGY), which serves as an injector to the 20-GeV Stanford linear accelerator, is based on photoionization of a polarized Li^6 atomic beam by a pulsed uv light source.[3] Typical characteristics of the polarized electron beam are given in Table I. The electron polarization, P_e, was measured by Mott scattering at the output of PEGGY and by Møller scattering at high energy. The value given for P_e is based on the Møller scattering measurements.[4,5] The uncertainty, $\delta P_e/P_e = 12\%$, includes counting statistics (10%) and the uncertainty in the uv light intensity for photoionization. (The polarization depends upon light intensity through a depolarizing resonant two-photon ionization process.[6])

Protons were polarized by the method of dynamic nuclear orientation in a butanol target doped with 1.4% porphyrexide.[7] Typical operating conditions are given in Table II. The techniques of beam rastering and target annealing[8] were used to reduce the effects of radiation damage to an acceptable level. Targets were annealed about every two hours and replaced after about five exposures to the beam. The continuously

TABLE I. Characteristics of polarized electron beam.

Characteristic	Value
Pulse length	1.5 μsec
Repetition rate	120 pulses/sec
Electron intensity (at high energy)	$\sim 10^9 e^-$/pulse
Pulse-to-pulse intensity variation	< 5%
Electron polarization, P_e	0.51 ± 0.06
Polarization reversal time	3 sec
Time between reversals	2 min
Intensity difference upon reversal	< 5%
Lifetime of lithium oven load	70 hr
Time to reload system	36 hr

TABLE II. Operating characteristics of polarized proton target.

Characteristic	Value
Magnetic field (longitudinal field of superconducting magnet)	50 kG
Temperature	1.05 K
Target material	25 cm^3 of butanol-porphyrexide beads (~1.7 mm diam)
Initial polarization of free protons[a]	0.50 to 0.65
Depolarizing dose (1/e)	$\sim 3\times 10^{14} e^-/cm^2$
Polarizing time (1/e)	~4 min
Anneal or target change time (including polarizing)	~45 min

[a]Improvements in target operation gave the larger polarization values in the later parts of the experiment.

monitored NMR signal normalized to a thermal equilibrium (TE) signal was used to determine the average target polarization P_p. The uncertainty, $\delta P_p/P_p = 10\%$, includes the errors in the TE measurements (8%) and the uncertainty in the correction for nonuniform irradiation of the target (5%). (Only ~70% of the total 2.5-cm × 2.5-cm target cross-sectional area was illuminated by the rastered electron beam.)

The electron beam from the accelerator was momentum-analyzed by a transport system whose absolute momentum calibration was ~0.1%. A momentum slit in the transport system limited the beam energy spread to ±0.375%. Spin precession in the 24.5° bend of the beam switchyard determined that only electrons whose energies were integral multiples of 3.237 GeV had full longitudinal polarization. The electron beam charge per pulse was monitored with two precision toroidal charge monitors. Just upstream of the target, a microwave beam position monitor measured the beam position for each beam pulse with a sensitivity of ~0.1 mm. Computer-controlled vernier steering magnets 99 m upstream of the target were used in conjunction with this position monitor to keep the raster pattern of the beam centered on the target.

The scattered electrons were detected and their momentum and scattering angle were measured with the Stanford Linear Accelerator Center (SLAC) 8-GeV spectrometer. Electron identification was achieved with a gas threshold Cherenkov counter, a 3.25-radiation-length-thick lead glass counter array which sampled the buildup of the electromagnetic shower, and a lead-Isolite[9] shower counter. Less than one pion in 10^3 was misidentified as an electron by this system. An on-line XDS 9300 computer monitored the experiment and wrote data on magnetic tape.

Data were taken in a series of runs, each of which lasted about two hours. Runs were terminated when radiation damage reduced the target polarization to about half its initial value. The proton polarization direction was constant during a run and was reversed between runs. Each run was divided into cycles, with each cycle in turn comprising eight miniruns of about one-minute duration each. The electron polarization direction remained constant during a minirun and was varied in the pattern $--++--++$, where $-$ ($+$) refers to the electron having negative (positive) helicity in the accelerator. This rapid modulation of the electron beam helicity was an important factor in avoiding systematic errors in the asymmetry measurement.

Each target raster pattern consisted of 313 points and was completed in 2.6 sec. An integral number of raster patterns was used for each minirun. The number of events taken in each minirun was normalized to the total charge measured by the toroids, and corrections were made for losses due to computer sampling, multiple hodoscope tracks, and dead time. The experimental asymmetry, Δ, is the quantity $\pm[(1256)-(3478)]/[(1256)+(3478)]$, where (1256) and (3478) refer to the sums of the corrected and normalized number of events in miniruns 1, 2, 5, 6 and 3, 4, 7, 8, respectively. The sign of Δ is chosen to give the antiparallel-minus-parallel asymmetry in accordance with Eq. (1). False asymmetries were measured with other combinations of miniruns.

Elastic scattering data were taken at the kinematic point for which $E = 6.473$ GeV, $E' = 6.066$ GeV, $\theta = 8.005°$, and $Q^2 = 0.765$ $(\mathrm{GeV}/c)^2$. A total of 2.1×10^6 electrons were detected with a typical

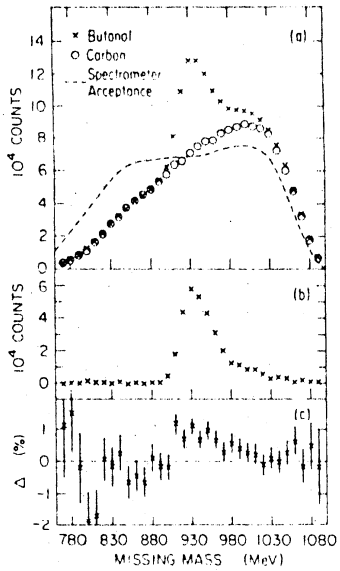

FIG. 1. Elastic scattering results for $E = 6.473$ GeV, $\theta = 8.005°$; (a) scattered electron counts versus missing mass with calculated spectrometer acceptance in arbitrary units; (b) scattered electron counts from free protons versus missing mass; (c) experimental asymmetry Δ versus missing mass.

counting rate of 0.25 scattered electrons per 1.5 μsec beam pulse. The combined missing mass (W) spectrum for electrons scattered from butanol for all runs independent of beam or target polarization is shown in Fig. 1(a), together with the background from electron-carbon scattering normalized to equal areas in the mass region $720 \leq W < 880$ MeV. Also shown in Fig. 1(a) is the spectrometer acceptance as determined from a Monte Carlo ray-tracing calculation. The free-proton spectrum (butanol minus background) versus missing mass is shown in Fig. 1(b). The experimental asymmetry, Δ, is shown plotted versus W in Fig. 1(c). The positive asymmetry associated with elastic scattering from free protons is apparent. Values of Δ for three missing-mass regions are given in Table III. Several false asymmetries, calculated over the complete missing-mass region 720 MeV $\leq W \leq$ 1120 MeV, are shown in Table IV, together with the χ^2 values for the agreement with zero of the measured false asymmetries for the 21 individual runs. No statistically significant false asymmetry was found.

The differential-cross-section asymmetry A of Eq. (1) is related to Δ by

$$\Delta = P_e P_p F A. \tag{3}$$

ere F is the fraction of scattered electrons

TABLE III. Experimental asymmetry, Δ.

W (MeV)	Δ (%)
$720 \leq W < 890$	-0.36 ± 0.18
$890 \leq W < 1000$	$+0.63 \pm 0.10$
$1000 \leq W < 1120$[a]	$+0.15 \pm 0.13$

[a]Since a small fraction of the scattering events from free protons fall in this region, an asymmetry Δ of about +0.13% is expected.

within the elastic missing-mass region ($890 \leq W < 1000$ MeV) which originate from free protons. Using the normalized carbon spectrum to determine the bound-nucleon background, we obtained a value of $F = 0.27 \pm 0.02$. To obtain A, we could have used Eq. (3) with $P_e = 0.51$, the average value of $P_p \simeq 0.34$, and $\Delta = 0.0063 \pm 0.0010$ within the elastic region (Table III). Instead, we used a somewhat different method of calculation which took into account the gradual decrease of the target polarization during a run. Our final result is $A = 0.138 \pm 0.031$ (0.019), where the statistical counting error, shown in parentheses, is added in quadrature to the systematic errors in P_e, P_p, and F to determine the total uncertainty. The values obtained for Δ with the two different directions of proton polarization agree within statistical counting errors. This agreement provides an important test of the validity of our result. Systematic errors in Δ arising from a correlation of beam energy or angle with beam helicity are small compared to the statistical error, as is the error associated with the measurement of beam charge by the toroids. The effect of radiative corrections on A is expected to be small, and these corrections to the data have not yet been made.

The theoretical expression for A of Eq. (2) de-

TABLE IV. False asymmetries.

Combination of miniruns	Average asymmetry[a] (%)	$\chi^2(0)$ per degree of freedom
$\frac{(1234)-(5678)}{(1234)+(5678)}$	0.02 ± 0.07	13/21
$\frac{(1357)-(2468)}{(1357)+(2468)}$	0.01 ± 0.07	18/21
$\frac{(2367)-(1458)}{(2367)+(1458)}$	-0.08 ± 0.07	17/21

[a]Independent of sign of P_p.

pends on both the magnitude and sign of G_E/G_M. Unpolarized elastic scattering experiments determine G_E^2 and G_M^2, but not the sign of G_E/G_M.

r $Q^2 = 0.765$ (GeV/c)^2 these experiments[10] give $|\mu G_E/G_M| = 0.98 \pm 0.04$ in which $\mu = 2.79$. If G_E and G_M have the same sign, Eq. (2) yields $A = +0.112 \pm 0.001$, while if G_E and G_M have the opposite sign Eq. (2) gives $A = -0.017 \pm 0.002$. From our measured value of A we conclude that the theoretical and experimental values are in good agreement provided the signs of G_E and G_M are the same. The effect of proton structure on the hyperfine-structure interval in hydrogen involves an integral of the product of the proton structure functions and also gives the sign of G_E/G_M to be positive.[11]

The experimental method described in this Letter could in principle[2,12] be applied to determine G_E in the region $Q^2 \gtrsim 2$ (GeV/c)^2, where G_E is not well known, but its practical usefulness is limited by low counting rates.

We are happy to acknowledge the important contributions to this experiment by M. Browne, S. Dhawan, R. Eisele, Z. Farkas, R. Fong-Tom, H. Hogg, E. Garwin, R. Koontz, J. Sodja, S. St. Lorant, J. Wesley, and M. Zeller.

Research supported in part by the U. S. Energy Research and Development Administration under Contract No. E(11-1)-3075 (Yale) and Contract No. E(04-3)-515, (Stanford Linear Accelerator Center), the German Federal Ministry of Research and Technology, and the University of Bielefeld, the Japan Society for the Promotion of Science, and the National Science Foundation.

[1]M. J. Alguard *et al.*, following Letter [Phys. Rev. Lett. 37, 1261 (1976)].

[2]N. Dombey, Rev. Mod. Phys. 41, 236 (1969). The methodology of this paper was used to derive Eq. (2).

[3]V. W. Hughes *et al.*, Phys. Rev. A 5, 195 (1972); M. J. Alguard *et al.*, in *Proceedings of the Ninth International Conference on High Energy Accelerators, Stanford Linear Accelerator Center, Stanford, California, 1974*, CONF-740 522 (National Technical Information Service, Springfield, Va., 1974), p. 309.

[4]P. S. Cooper *et al.*, Phys. Rev. Lett. 34, 1589 (1975).

[5]We thank the members of SLAC Group A for their invaluable help in making the electron polarization measurement by Møller scattering in March 1976.

[6]M. J. Alguard *et al.*, Bull. Am. Phys. Soc. 21, 98 (1976).

[7]W. W. Ash, in Proceedings of the Brookhaven National Laboratory Workshop in Physics with Polarized Targets, June 1974, BNL Report No. 20415 (unpublished), p. 309; W. W. Ash *et al.*, to be published.

[8]M. Borghini *et al.*, Nucl. Instrum. Methods 84, 168 (1970).

[9]Isolite is the name for a plastic formed by adding a wavelength-shifter to Lucite.

[10]Ch. Berger *et al.*, Phys. Lett. 35B, 87 (1971); W. Bartel *et al.*, Nucl. Phys. B 58, 429 (1973).

[11]H. Grotch and D. R. Yennie, Rev. Mod. Phys. 41, 350 (1969); C. Zemach, Phys. Rev. 104, 1771 (1956).

[12]A. I. Akhiezer *et al.*, Zh. Eksp. Teor. Fiz. 33, 765 (1957) [Sov. Phys. JETP 6, 588 (1958)].

VOLUME 37, NUMBER 19 PHYSICAL REVIEW LETTERS 8 NOVEMBER 1976

Deep Inelastic Scattering of Polarized Electrons by Polarized Protons*

M. J. Alguard, W. W. Ash, G. Baum, J. E. Clendenin, P. S. Cooper, D. H. Coward, R. D. Ehrlich, A. Etkin, V. W. Hughes, H. Kobayakawa, K. Kondo, M. S. Lubell, R. H. Miller, D. A. Palmer, W. Raith, N. Sasao, K. P. Schüler, D. J. Sherden, C. K. Sinclair, and P. A. Souder

University of Bielefeld, Bielefeld, West Germany, and City University of New York, New York, New York 10031, and Nagoya University, Nagoya, Japan, and Stanford Linear Accelerator Center, Stanford, California 94305, and University of Tsukuba, Ibaraki, Japan, and Yale University, New Haven, Connecticut 06520

(Received 5 August 1976)

We report measurements of the asymmetry in deep inelastic scattering of longitudinally polarized electrons by longitudinally polarized protons. The antiparallel-parallel asymmetries are positive and large in agreement with predictions of quark-parton models of the proton. A limit is obtained on parity nonconservation in the scattering of longitudinally polarized electrons by unpolarized nucleons.

Experimental and theoretical studies of deep inelastic electron scattering from protons and neutrons have led in the past eight years to the important discovery of scaling and to the quark-parton model of nucleon structure.[1] Deep inelastic muon[2] and neutrino[3] scattering have confirmed these general ideas.[4]

For deep inelastic electron-proton scattering,

accurate data have been obtained on the differential cross section $d^2\sigma/d\Omega dE'$ over a wide range of the energy loss, ν, of the electron and the square of the four-momentum transfer, q^2, to the proton. The two spin-averaged proton structure functions $W_1(\nu,q^2)$ and $W_2(\nu,q^2)$ have been determined from these data. Important, independent information is contained in two additional spin-dependent proton structure functions whose determination requires the measurement of spin correlation asymmetries.[5]

In this Letter we report the first results of an experiment done at the Stanford Linear Accelerator Center (SLAC) to measure the asymmetry, A, in the deep inelastic scattering of longitudinally polarized electrons by longitudinally polarized protons, where A is given by

$$A=[d\sigma(\uparrow\downarrow)-d\sigma(\uparrow\uparrow)]/[d\sigma(\uparrow\downarrow)+d\sigma(\uparrow\uparrow)], \tag{1}$$

with $d\sigma$ denoting the differential cross section $d^2\sigma(E,E',\theta)/d\Omega dE'$ for electrons of incident (scattered) energy E (E') and laboratory scattering angle θ, and the arrows denoting the antiparallel and parallel spin configurations.

If the scattering is described by the one-photon-exchange approximation, then for unpolarized electrons the virtual photons are linearly polarized, whereas for polarized electrons the photons are elliptically polarized. The differential cross section for the scattering of longitudinally polarized electrons by longitudinally polarized protons is

$$\frac{d^2\sigma}{d\Omega dE'}=\left(\frac{d\sigma}{d\Omega}\right)_M\left(\frac{1}{\epsilon(1+\nu^2/Q^2)}\right)W_1\{1+\epsilon R\pm(1-\epsilon^2)^{1/2}\cos\psi A_1\pm[2\epsilon(1-\epsilon)]^{1/2}\sin\psi A_2\}, \tag{2}$$

in which $(d\sigma/d\Omega)_M$ is the Mott differential cross section, $\epsilon=[1+2(1+\nu^2/Q^2)\tan^2\frac{1}{2}\theta]^{-1}$, $Q^2=-q^2$, $R=\sigma_L/\sigma_T$ is the ratio of the cross sections for absorption of longitudinal and transverse virtual photons, and ψ is the angle between the directions of the virtual photon momentum and the proton spin. The + (−) signs in Eq. (2) refer to the antiparallel (parallel) spin configurations.

The spin-dependent terms A_1 and A_2 are two new measurable quantities which can be expressed in terms of two spin-dependent structure functions.[5,6] Equivalently, they can be expressed in terms of the total absorption cross sections of circularly polarized photons on polarized protons as

$$A_1=(\sigma_{1/2}-\sigma_{3/2})/(\sigma_{1/2}+\sigma_{3/2}),$$
$$A_2=2\sigma_{TL}/(\sigma_{1/2}+\sigma_{3/2}), \tag{3}$$

where $\sigma_{1/2}$ ($\sigma_{3/2}$) is the total absorption cross section when the z component (z is the direction of the virtual photon momentum) of angular momentum of the virtual photon plus proton is $\frac{1}{2}$ ($\frac{3}{2}$), and σ_{TL}, which may be negative, is a term which arises from the interference between transverse and longitudinal photon-nucleon amplitudes. It should be noted that $\sigma_{1/2}$ and $\sigma_{3/2}$ are related to σ_T by $\sigma_{1/2}+\sigma_{3/2}=2\sigma_T$.

For the case of protons polarized along the incident beam direction, the asymmetry A of Eq. (1) is

$$A=D(A_1+\eta A_2), \tag{4}$$

where

$$D=(E-E'\epsilon)/E(1+\epsilon R)$$
$$=(1-\epsilon^2)^{1/2}\cos\psi/(1+\epsilon R), \tag{5}$$

and

$$\eta=\epsilon(Q^2)^{1/2}/(E-E'\epsilon)$$
$$=[2\epsilon/(1+\epsilon)]^{1/2}\tan\psi\simeq\tan\psi. \tag{6}$$

The quantity D can be regarded as a kinematic depolarization factor of the virtual photon and is ~0.3 for our kinematic points. Positivity limits imposed on A_1 and A_2 are[7]

$$|A_1|\leq 1,\quad |A_2|\leq\sqrt{R}. \tag{7}$$

In this experiment we determine the combination $A_1+\eta A_2$ by dividing the measured electron-proton asymmetry A by the depolarization factor D. Although we do not separately determine A_1 and A_2, our result is dominated by A_1 because the kinematic factor η is small.

On the basis of a high-energy sum rule derived with the algebra of currents for a quark model, it has been predicted[8] that A_1 has a positive value greater than 0.2 over a large region of the deep inelastic continuum. Scaling relations are predicted for the spin-dependent proton structure functions, and hence also for A_1[9]:

$$A_1(\nu,Q^2)\to A_1(\omega)\text{ as }\nu,Q^2\to\infty,\text{ with }\omega\text{ held constant} \tag{8}$$

($\omega=2M\nu/Q^2$, M is the proton mass). Specific models of proton structure make widely varying predictions for A_1. The simplest quark-parton

TABLE I. Results of asymmetry measurements.

E (GeV)	θ (deg)	Q^2 [(GeV/c)^2]	W[a] (GeV)	ω	Δ (%)	A[b]	D[c]	$A_1+\eta A_2$[b]	$\lvert\eta A_2\rvert$
9.711	9.000	1.680	2.059	3	0.44 ± 0.11	0.191 ± 0.057 (0.044)	0.284	0.67 ± 0.20 (0.16)	< 0.146
12.948	9.000	2.735	2.519	3	0.50 ± 0.17	0.215 ± 0.089 (0.080)	0.352	0.61 ± 0.25 (0.23)	< 0.109
9.711	9.000	1.418	2.560	5	0.28 ± 0.11	0.141 ± 0.058 (0.051)	0.412	0.34 ± 0.14 (0.12)	< 0.087

[a] W is the missing mass of undetected hadron system.
[b] The total errors are the statistical counting errors added in quadrature to the systematic errors in P_e, P_p, and F; the numbers in parentheses are the 1-standard-deviation counting errors.
[c] D is obtained from Eq. (5) using $R = 0.14$.

model predicts that $A_1 = \frac{5}{9}$, and more elaborate models also predict large positive values for $A_1(\omega)$.[5,10]

The method of measuring the experimental asymmetry, Δ, for deep inelastic electron-proton scattering was the same as that described for elastic scattering in the preceding Letter.[11] For the inelastic case, the scattered electron counting rate was lower (0.02 to 0.06 electrons per pulse).

TABLE II. False asymmetries.[a]

Combination of miniruns	Average asymmetry[b] (%)	$\chi^2(0)$ per degree of freedom
	$\omega = 3$, $Q^2 = 1.680$	
$\frac{(1234)-(5678)}{(1234)+(5678)}$	0.04 ± 0.11	18/34
$\frac{(1357)-(2468)}{(1357)+(2468)}$	−0.04 ± 0.11	38/34
$\frac{(2367)-(1458)}{(2367)+(1458)}$	+0.14 ± 0.11	27/34
	$\omega = 3$, $Q^2 = 2.735$	
$\frac{(1234)-(5678)}{(1234)+(5678)}$	−0.30 ± 0.17	33/30
$\frac{(1357)-(2468)}{(1357)+(2468)}$	−0.03 ± 0.17	26/30
$\frac{(2367)-(1458)}{(2367)+(1458)}$	+0.24 ± 0.017	40/30
	$\omega = 5$, $Q^2 = 1.418$	
$\frac{(1234)-(5678)}{(1234)+(5678)}$	−0.12 ± 0.11	34/35
$\frac{(1357)-(2468)}{(1357)+(2468)}$	−0.10 ± 0.11	34/35
$\frac{(2367)-(1458)}{(2367)+(1458)}$	−0.03 ± 0.11	30/35

[a] See preceding Letter (Ref. 11) for definitions of false asymmetries.
[b] Irrespective of sign of target polarization.

Background due to misidentified pions was again negligible.

The antiparallel-parallel asymmetry Δ was measured for three deep inelastic kinematic points and the results are given in Table I. Several false asymmetries were also measured and are listed in Table II, together with the χ^2 values for the agreement with zero of the measured false asymmetries for the indicated degrees of freedom (number of individual runs). No statistically significant false asymmetries were found.

The asymmetry A of Eq. (1) is related to Δ by

$$\Delta = P_e P_p F A. \tag{9}$$

The electron polarization, P_e, was 0.51 ± 0.06, and the average target polarization, P_p, measured for each kinematic point, was ≃ 0.40 with 10% uncertainty. The quantity F is the fraction of detected electrons scattered from free protons. This is taken as the ratio of the number of free protons to the total number of nucleons in the target, including measured contributions from helium and other background sources. A small correction for the difference in scattering cross sections of neutrons and protons was also included. The value for F, determined for each point, was ≃ 0.11 with a 10% uncertainty.

The measured values of A are listed in Table I. The uncertainties are dominated by counting statistics. No radiative corrections have yet been made. Also listed are the quantities D (evaluated using $R = 0.14$),[1] $A/D = A_1 + \eta A_2$, and upper limits for $|\eta A_2|$ (taking $A_2 = \sqrt{R}$). From Table I it is seen that A/D is dominated by A_1. Furthermore, parton theories predict[12] that the interference term A_2 will be considerably smaller than its positivity limit $\sqrt{R}$. It is therefore valid to compare our measured value of A/D to theoretical predictions for A_1 as shown in Fig. 1.

With the explicit assumption that $A/D = A_1$, our

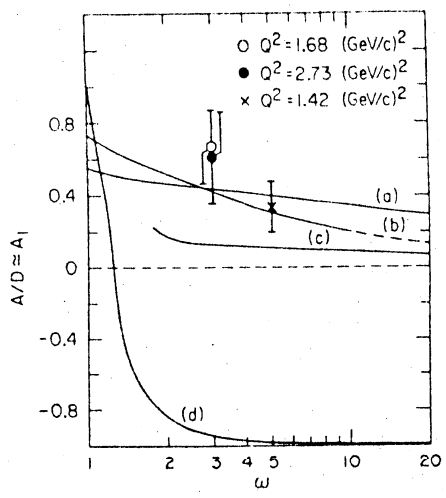

FIG. 1. Experimental values of $A/D \approx A_1$ and theoretical predictions of the virtual-photon–proton asymmetry A_1 versus ω. Theoretical curves a, b, c, and d are obtained from Refs. 5, 10, 13, and 14, respectively. For curve c the quark model with symmetry breaking is used: The model does not give values for A_1 in the range $1 < \omega < 2$, but rather gives $A_1(1) = 1$. For curve d the quantity $\mu^2/m_\rho{}^2$ in the theory is taken equal to 0.12.

values of A_1 are indeed positive and large in accord with early theoretical expectations from sum rules.[8] The two values for $\omega = 3$ agree within their errors, which is consistent with the expectation that A_1 satisfies the scaling relation, given by Eq. (8). Our data are consistent with the predictions of the quark-parton models shown as curves a [5] and b [10] in Fig. 1, but disagree strongly with the resonance model[13] (curve c) and the bare-nucleon–bare-meson model[14] (curve d). We note that the theoretical curves are all given for the scaling limit.

Data from this experiment can also be used to place a limit on parity nonconservation in the scattering of longitudinally polarized electrons from unpolarized nucleons, i.e., an interaction term of the form $\vec{\sigma}_e \cdot \vec{p}_e$ in which $\vec{\sigma}_e$ is the electron spin and $\vec{p}_e$ is the electron incident momentum. If we define Δ^+ (Δ^-) as the asymmetry for protons polarized along (against) the beam direction and if the magnitude of P_p is the same for both cases, then we can define an asymmetry, $\Delta_{\rm PNC}$, associated with parity nonconservation by[15]

$$\Delta_{\rm PNC} = (\Delta^+ - \Delta^-)/2 \equiv r P_e, \qquad (10)$$

in which $r = (d\sigma^- - d\sigma^+)/(d\sigma^- + d\sigma^+)$ is the asymmetry for electron polarization $P_e = 1$, and the minus and plus superscripts refer to the electron beam helicity. From the deep inelastic scattering data summarized in Table I for Q^2 between 1.4 and 2.7 $(\mathrm{GeV}/c)^2$, we find that r is consistent with zero. For the combined data we have an upper limit of $r < 5 \times 10^{-3}$ with a 95% confidence level. For the elastic scattering data reported in the preceding Letter,[11] again r is consistent with zero and its upper limit is less than 3×10^{-3} with a 95% confidence level. The gauge theories of weak and electromagnetic interactions, which contain parity nonconservation, predict[16,17] considerably smaller values of $r \simeq (10^{-5}$ to $10^{-4}) Q^2/M^2$.

We are happy to acknowledge helpful and stimulating discussions with J. D. Bjorken, F. Gilman, and J. Kuti.

---

*Research supported in part by the U. S. Energy Research and Development Administration under Contract No. E(11-1)-3075 (Yale) and Contract No. E(04-3)-515 (Stanford Linear Accelerator Center), the German Federal Ministry of Research and Technology and the University of Bielefeld, the Japan Society for the Promotion of Science, and the National Science Foundation.

[1]R. E. Taylor, in *Proceedings of the International Symposium on Lepton and Photon Interactions at High Energies, Stanford, California, 1975*, edited by W. T. Kirk (Stanford Linear Accelerator Center, Stanford, Calif., 1975), p. 679. See also references therein.

[2]L. Mo, in *Proceedings of the International Symposium on Lepton and Photon Interactions at High Energies, Stanford, California, 1975*, edited by W. T. Kirk (Stanford Linear Accelerator Center, Stanford, Calif., 1975), p. 651.

[3]D. H. Perkins, in *Proceedings of the International Symposium on Lepton and Photon Interactions at High Energies, Stanford, California, 1975*, edited by W. T. Kirk (Stanford Linear Accelerator Center, Stanford, Calif., 1975), p. 571.

[4]C. H. Llewellyn-Smith, in *Proceedings of the International Symposium on Lepton and Photon Interactions at High Energies, Stanford, California, 1975*, edited by W. T. Kirk (Stanford Linear Accelerator Center, Stanford, Calif., 1975), p. 709. See also references therein.

[5]J. Kuti and V. F. Weisskopf, Phys. Rev. D 4, 3418 (1971).

[6]F. Gilman, Phys. Rep. 4, 95 (1972); F. Gilman, SLAC Report No. SLAC-167, 1973 (unpublished), Vol. I, p. 71.

[7]M. G. Doncel and E. de Rafael, Nuovo Cimento 4A, 363 (1971).

[8]J. D. Bjorken, Phys. Rev. D 1, 1376 (1970).

[9]L. Galfi *et al.*, Phys. Lett. 31B, 465 (1970).

[10]F. Close, Nucl. Phys. B80, 269 (1974), and references therein.

[11]M. J. Alguard *et al.*, preceding Letter [Phys. Rev.

Lett. 37, 1258 (1976)].
[12]J. D. Bjorken and F. Gilman, private communication.
[13]G. Domokos *et al.*, Phys. Rev. D 3, 1191 (1971).
[14]S. D. Drell and T. D. Lee, Phys. Rev. D 5, 1738 (1972).
[15]In the actual analysis, target polarization differences were included. Since $P_p FA \simeq 0.01$ is small, these differences have little effect.
[16]S. M. Berman and J. R. Primack, Phys. Rev. D 9, 2171 (1974).
[17]G. Feinberg, Phys. Rev. D 12, 3575 (1975).

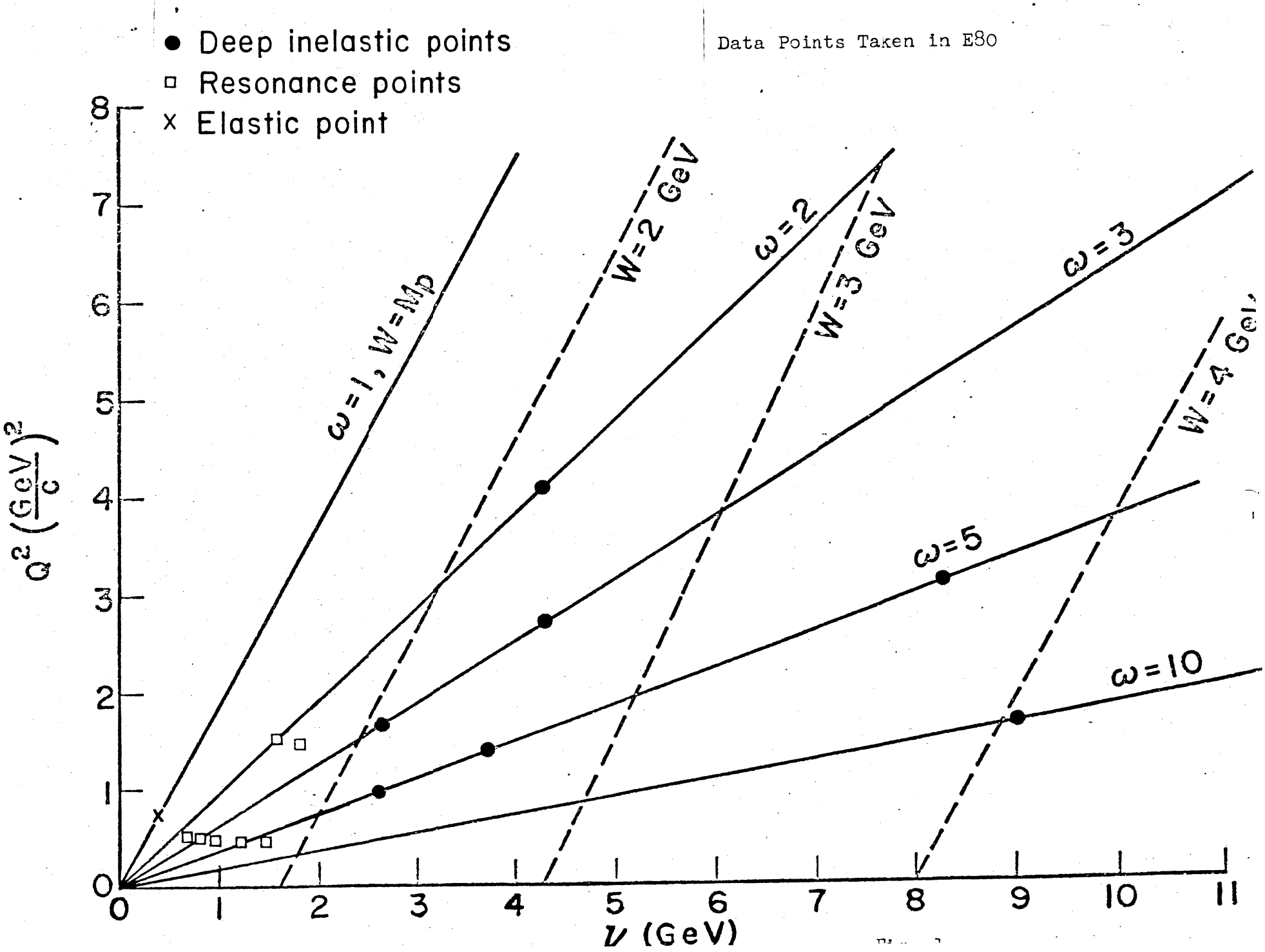
Deep inelastic points
Resonance points
Elastic point
Data Points Taken in E80
$Q^2\left(\frac{GeV}{c}\right)^2$
ν (GeV)
$\omega=1$, $W=M_p$
$W=2$ GeV
$\omega=2$
$W=3$ GeV
$\omega=3$
$W=4$ GeV
$\omega=5$
$\omega=10$
0
1
2
3
4
5
6
7
8
9
10
11

Table Results of Asymmetry Measurements in De Inelastic Scattering (Data taken in 19[illegible] [Published in Phys. Rev. Lett. 37, 1261 (1976)]

E (GeV)	θ (deg)	Q^2 $(GeV/c)^2$	W (GeV)	ω	Δ(%)	A[a]	D[b]	$A_1 + \eta A_2$[a]	$\lvert\eta A_2\rvert$[c]
9.71	9°	1.680	2.059	3	0.44±0.11	0.191±0.057(0.044)	0.284	0.67±0.20(0.16)	<0.146
12.95	9°	2.735	2.519	3	0.50±0.17	0.215±0.089(0.080)	0.352	0.61±0.25(0.23)	<0.109
9.71	9°	1.413	2.560	5	0.28±0.11	0.141±0.058(0.051)	0.412	0.34±0.14(0.12)	<0.087

Preliminary On-line Results (Data taken in 1976)

E (GeV)	θ (deg)	Q^2 $(GeV/c)^2$	W (GeV)	ω	Δ(%)	A[a]	D[b]	$A_1 + \eta A_2$[a]	$\lvert\eta A_2\rvert$[c]
12.95	11°	4.09	2.22	2	1.03±0.27	0.173±0.054(0.0452)	0.35	0.49±0.15(0.13)	0.133
9.71	9°	1.68	2.06	3	0.72±0.19	0.173±0.054(0.045)	0.284	0.61±0.19(0.16)	0.146
12.95	9°	2.74	2.52	3	0.80±0.34	0.192±0.088(0.082)	0.352	0.55±0.25(0.23)	0.109
9.71	7°	1.02	2.20	4.9	0.34±0.11	0.086±0.031(0.027)	0.277	0.31±0.11(0.10)	0.117
16.18	8.5°	2.95	3.56	5	1.00±0.34	0.251±0.096(0.086)	0.527	0.48±0.18(0.16)	0.055
16.18	7°	1.70	4.04	10	0.46±0.18	0.115±0.050(0.045)	0.619	0.19±0.08(0.07)	0.032

a) The total errors are the statistical counting errors added in quadrature to the systematic errors in P_e, P_p and F; the numbers in parentheses are the one standard deviation counting errors.

b) $D = (E-E'\varepsilon)/E(1+\varepsilon R)$ with $R = 0.14$.

c) Upper limits for $|\eta A_2|$ taking $A_2 = \sqrt{R}$.

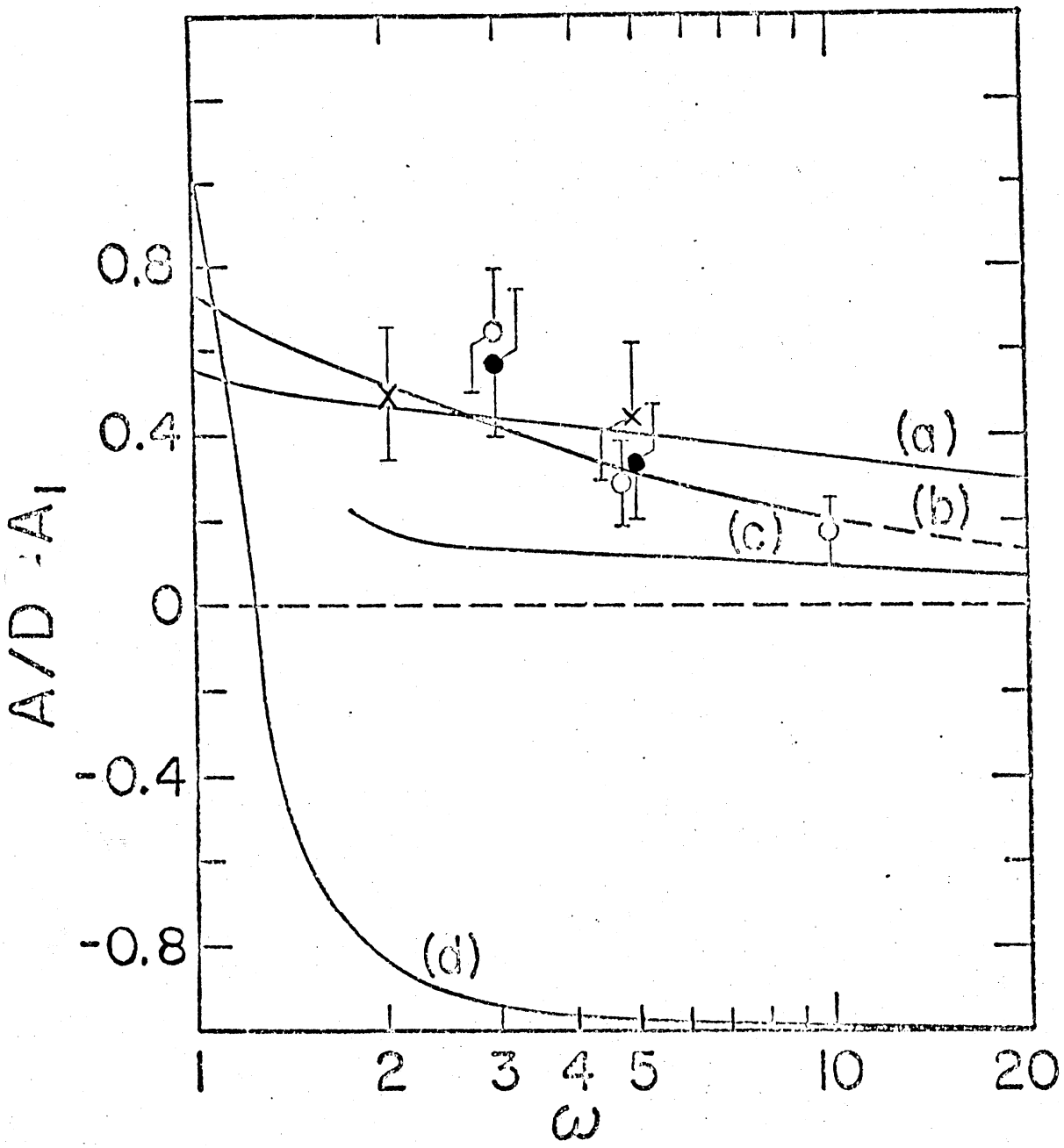

(See Fig. 1 of Phys. Rev. Lett. 37, 1261 (1976)
and Table 1, p. 8 of this proposal)

Fig. 2

Bjorken's sum rule

The Bjorken sum rule is an important general consequence of the quark-parton model of the nucleon and of the assumption that the weak current for quarks has the same form as that for leptons. (Bjorken, 1966, 1970; Feynman, 1972) It can be written

$$\int_0^1 \frac{dx}{x}\left[A_1^p(x) \cdot \nu W_2^p(x) - A_1^n(x) \cdot \nu W_2^n(x)\right] = \frac{1}{3}\left|\frac{g_A}{g_V}\right| \simeq 0.4 \qquad (1)$$

where g_A/g_V is the ratio of axial to vector weak coupling constants, and is about 1.2 experimentally.

In order to evaluate the left hand side of the above equation, we assume

$$A_1^n(x) = 0 \qquad \text{(neutron asymmetry)}$$

and use a fit for νW_2^p obtained from the SLAC-MIT experiments. We use our measured values of $A_1^p(x)$ as given in Table 1 and assume further that scaling is valid so that A_1^p depends only on x. Hence we obtain for the range of x from 0.1 to 0.5

$$\int_{0.1}^{0.5} \frac{dx}{x}\left[A_1^p(x)\ \nu W_2^p(x)\right] = 0.19 \pm 0.03$$

Fig. 3 shows νW_2^p, $\nu W_2^p/x$ and our data points for $A_1^p(x)$ as a function of x.

It is obvious that the integral is very sensitive to the lower limit but not to the upper limit. If we assume $A_1^p(x) = 1$ for the range from 0.5 to 1.0, then the contribution to the integral from this region is about 0.02. Therefore, roughly speaking, about 50% of the sum rule is saturated by the contribution from the proton in the range x = 0.1 ~ 1.0.

J.D. Bjorken, Phys. Rev. 148, 1467 (1966).
J.D. Bjorken, Phys. Rev. D 1, 1376 (1970).
R.P. Feynman, Photon-Hadron Interactions (W.A. Benjamin, Inc., 1972).

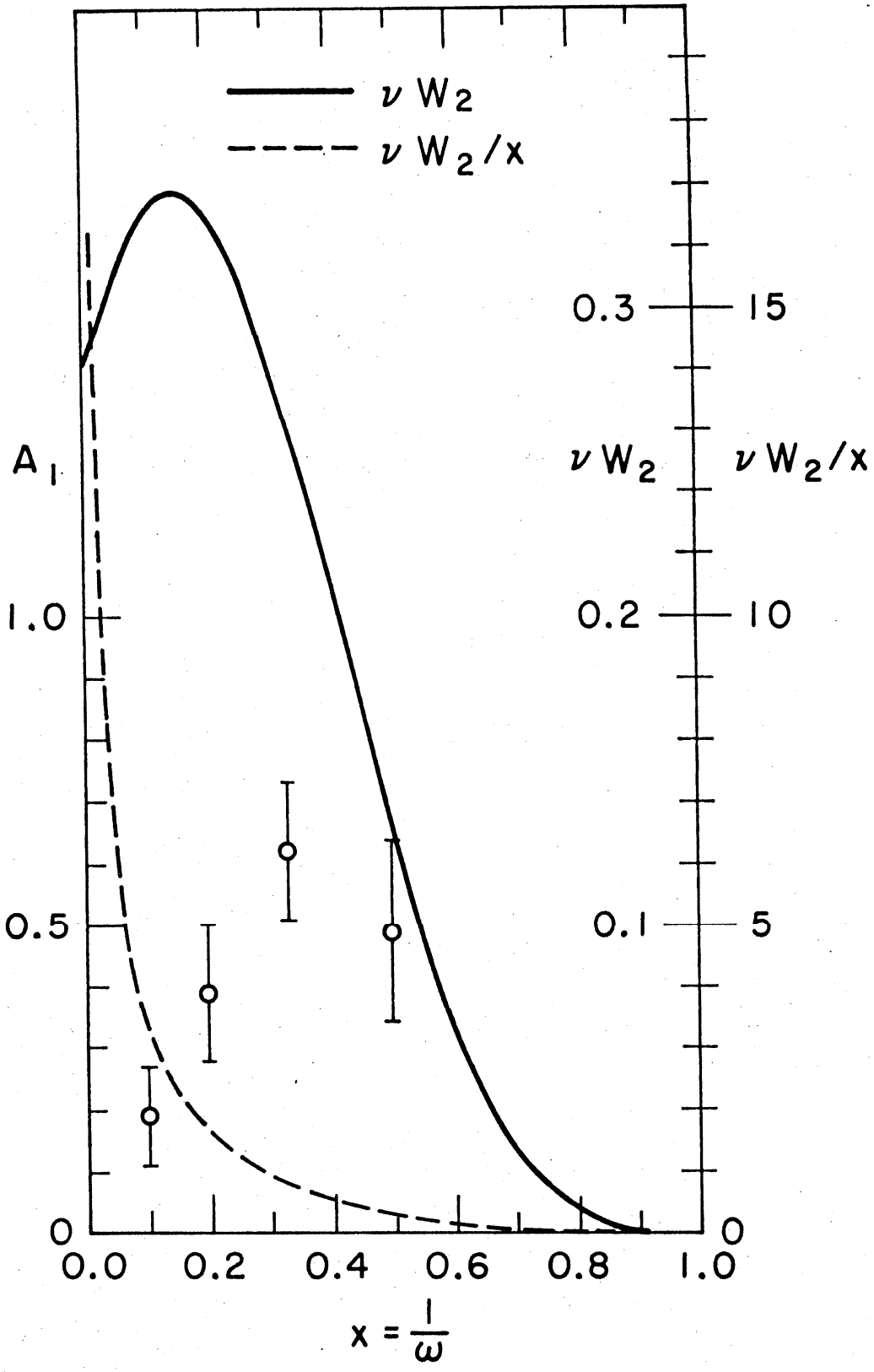

Graph relevant to Bjorken sum rule.

Fig. 3

Table 2. Preliminary On-line Results of Asymmetry Measurements in Resonance Region (Data Taken in 1976)

E (GeV)	θ (deg)	Q^2 $(GeV/c)^2$	W (GeV)	ω	Δ(%)	A^a	D^b	$A_1 + \eta A_2{}^a$
.47	7°	0.56	1.234	2.1	0.07±0.06	0.0135±0.0121(0.0110)	0.11	0.12±0.11(0.10)
.47	7°	0.55	1.376	2.9	0.27±0.11	0.0541±0.0243(0.0218)	0.14	0.38±0.17(0.15)
.47	7°	0.52	1.522	3.7	0.40±0.09	0.0799±0.0233(0.0180)	0.18	0.44±0.13(0.10)
.47	7°	0.50	1.688	5.0	0.26±0.08	0.0485±0.0175(0.0148)	0.23	0.21±0.08(0.06)
.47	7°	0.48	1.820	6.1	0.29±0.12	0.0541±0.0251(0.0228)	0.27	0.20±0.09(0.08)
.71	8°	1.54	1.522	1.9	0.58±0.13	0.1168±0.0339(0.0265)	0.18	0.64±0.18(0.14)
.71	8°	1.49	1.688	2.3	0.66±0.14	0.1085±0.0294(0.0228)	0.22	0.51±0.14(0.11)

a. The total errors are the statistical counting errors added in quadrature to the systematic errors in P_e, P_p and F; the number in parentheses are the one standard deviation counting errors.

b. $D = (E-E'\varepsilon)/E$; R is assumed to be 0.

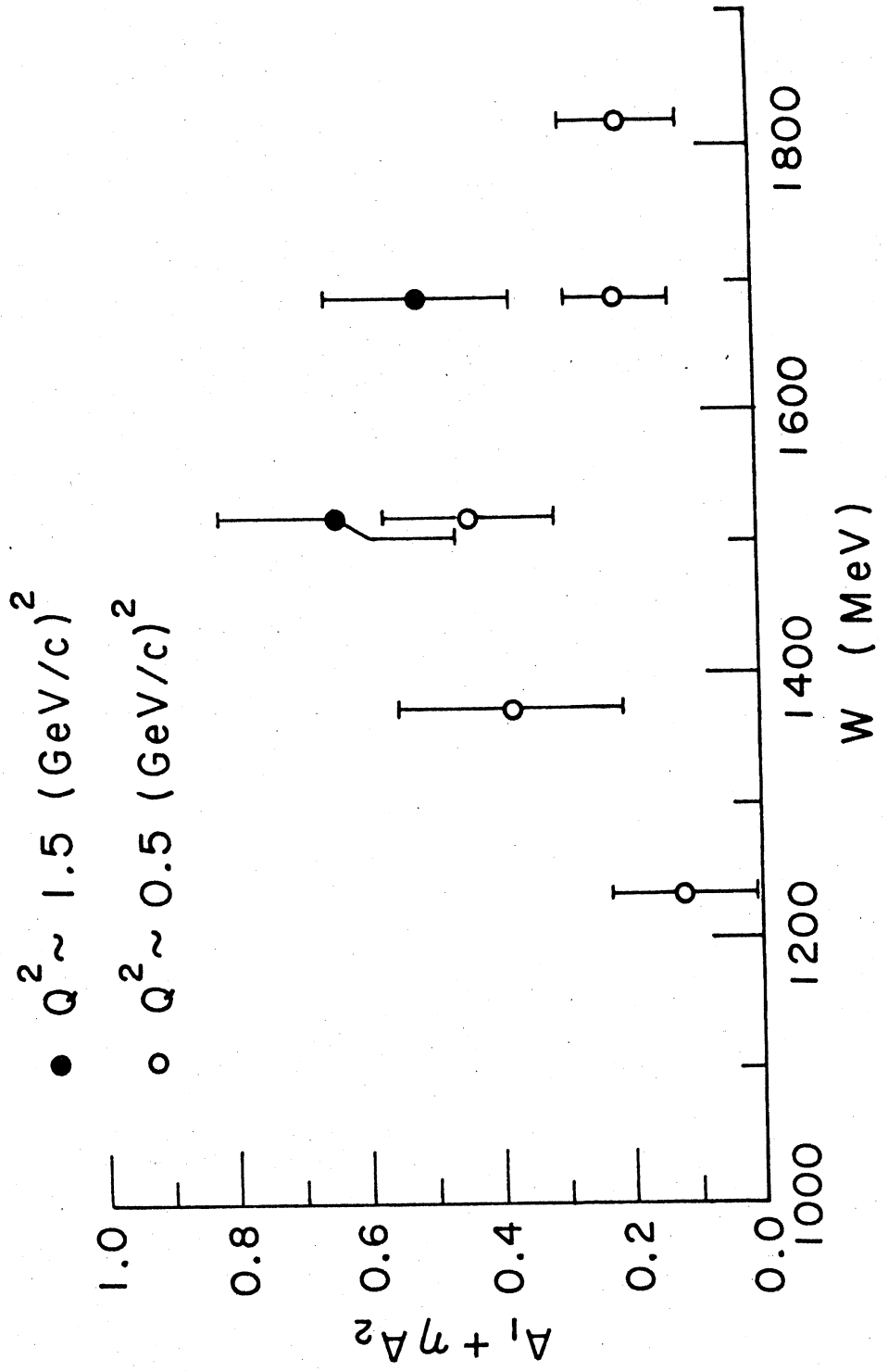

Fig. 4

One-Line Results in Resonance Region from E80.

II. Motivation

The principal scientific objectives of this proposal are (1) To increase the precision (~a factor of 3) and extend the kinematic range (ω ~ 1.5 to 13 and Q^2 up to 9 $(GeV/c)^2$) of measurement of the virtual photon-proton asymmetry A_1^p. These measurements will significantly improve the test of scaling for spin-dependent quantities and will provide useful results for distinguishing models of proton structure.

(2) To measure for the first time the virtual photon-neutron asymmetry A_1^n. Values of A_1^n very different from those of A_1^p are predicted by the theories of nucleon structure and will be tested by our measurements. Furthermore an improved test of the Bjorken sum rule (Eq.(1), p. 10) can be made when neutron data are available.

A new large acceptance spectrometer operating up to 18 GeV/c together with improvements in the beam intensity and target polarization will result in an effective increase in data accumulation rate by more than an order of magnitude. The statistical error in the counting rate asymmetry $\Delta(\Delta=P_e P_p F A)$ for a particular kinematic point will be reduced by a factor of 3 to 4 compared to E80, and data over a wide kinematic range will be obtained simultaneously (Section III).

Measurements of the neutron asymmetry A^n (or A_1^n) can be deduced from measurements on the deuteron and on the proton. With adequate precision the deuteron magnetic moment can be taken as the sum o the proton and neutron magnetic moments (The effect of the ^3D state

admixture in the deuteron can be neglected.), and hence $\Delta_n = \Delta_d - \Delta_p = P_e P_n F_n A^n$, where $P_n \sim P_d$. Since the neutron asymmetry A^n must be obtained essentially by subtraction of the proton asymmetry from the deuteron asymmetry, and since, furthermore, achievable deuteron polarizations in targets are about 22% whereas proton polarizations are about 80%, the measurement of neutron asymmetry is difficult and the projected statistical accuracies are $\Delta A_1^n \simeq 0.05$ to 0.1. (See Table 10)

(1) The Bjorken sum rule is given in Eq. (1) on p. 10. This important relation was derived from the quark-parton model of the nucleon and the assumption that the weak current for quarks has the same form as that for leptons. We give on p.10 the present state of the test of this relation based on our measurements of proton asymmetry A_1^p. The main contribution that our proposed E130 experiment will make to an improved test of the Bjorken sum rule will be in providing data on A_1^n, which appears in a term of the sum rule. The new values of A_1^p will be of higher precision and will cover a slightly larger range in ω than the E80 data, and hence will be of some value to the accurate evaluation of the integral, particularly when they are combined later with values of A_1^p at high ω from the planned CERN muon deep inelastic polarization experiment.

(2) Violation of Bjorken scaling for the spin independent nucleon structure functions, has been observed both in electron (Taylor, 1975) and in muon (Mo 1975) deep inelastic scattering. This is a topic of great theoretical importance (Llewellyn-Smith, 1975). Scaling relations are also predicted for the spin dependent proton structure functions [e.g., $A_1^p(\nu, Q^2) = A_1^p(\omega)$ $\nu \to \infty$; $Q^2 \to \infty$]. Since the spin dependent proton structure functions are independent of the spin-averaged structure functions, the scaling relation for A_1^p is a new, independent relation. Scaling violation for spin-dependent structure functions may occur due to parton structure

(Colglazier and Rajaraman, 1974), as a logarithmic violation in gauge theory (Ahmen and Ross, 1975), or through use of the wrong scaling variable It will be useful to have a more precise test of scaling for A_1^p, which E130 dat should provide. Furthermore, eventually the combination of precise E130 data with the CERN polarized muon data at high Q^2 will also be very valuable.

(3) Theoretical predictions for A_1^p and A_1^n are given in Figures 5 and 6 from a number of classes of quark-parton models of the nucleon.

Curve 1. A relativistic symmetric valence quark model (Kuti-Weisskopf, 1971)

Curves 2. Models of Kuti-Weisskopf type using other recent experimental da from e-p, e-n and ν-N scattering and dilepton production in pp collisions, and improved quark distribution functions. [(a) Blankenbecler et al., 1975: (b) McElhaney and Tuan, 1973: (c) Barger and Phillips, 1974.]

Curve 3. Unsymmetrical model for which $A^n \to 1$ as $x \to 1$ with single parton carrying the entire nucleon momentum (Feynman, 1972, Close, 1973). See also Flume-Gorczyca and Kitakado (1974) and Farrar and Jackson (1975). Farrar and Jackson emphasize the importance of polarized e-p scattering near x=1.

Curve 4. Nucleon model incorporating the Melosh transformation which distinguishes between constituent and current quarks (Close, 1974).

Curve 5. Asymmetry prediction based on source theory which does not use a parton picture. (Schwinger, 1976, 1977)

The usefulness of the new higher precision proton asymmetry data we propose as regards the proton models can be discussed for three different regions of x values.

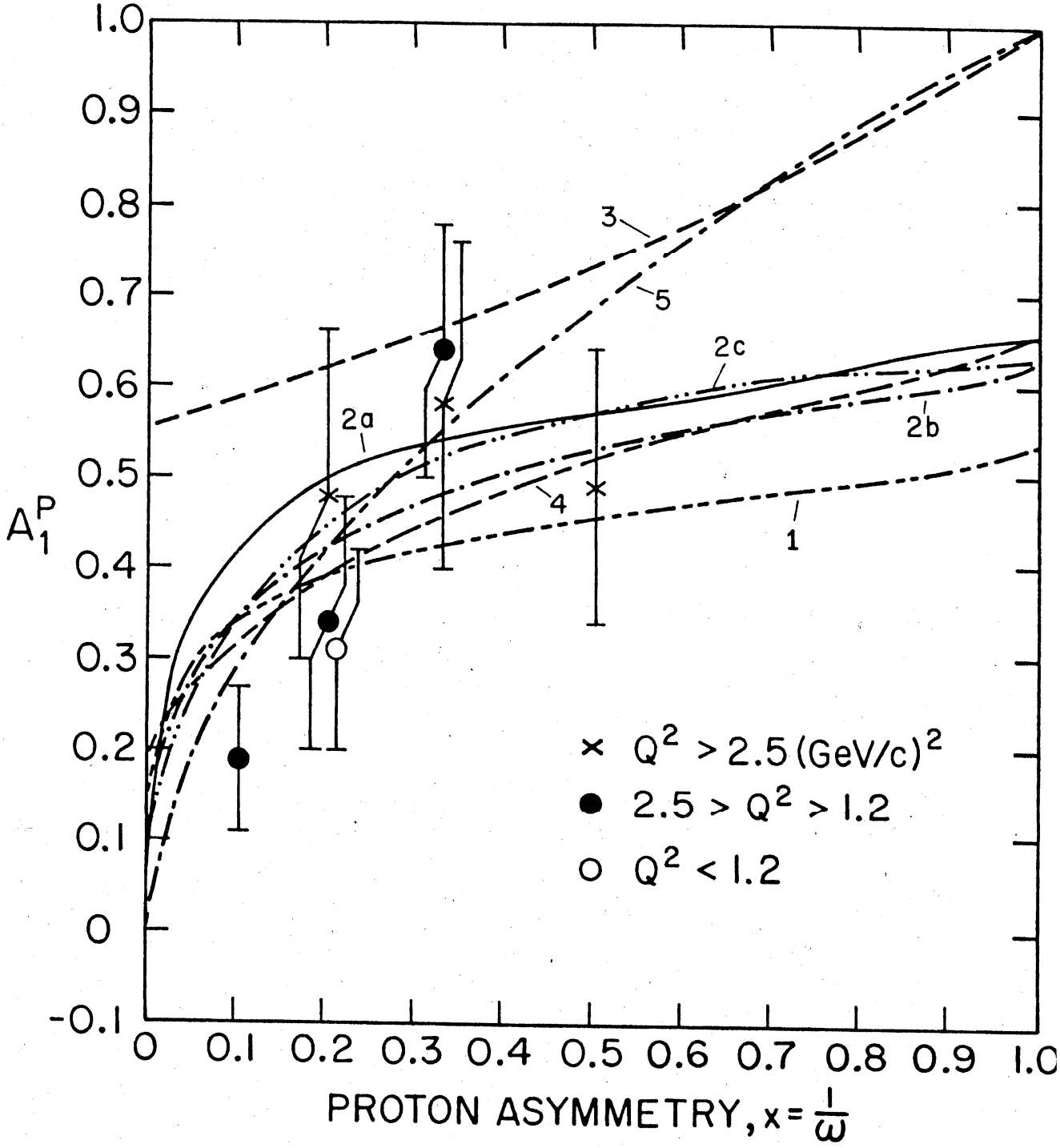
1.0
0.9
0.8
0.7
0.6
0.5
0.4
0.3
0.2
0.1
0
-0.1
A_1^P
0
0.1
0.2
0.3
0.4
0.5
0.6
0.7
0.8
0.9
1.0
PROTON ASYMMETRY, $x = \frac{1}{\omega}$
3
5
2c
2a
2b
4
1
× $Q^2 > 2.5$ (GeV/c)^2
● $2.5 > Q^2 > 1.2$
○ $Q^2 < 1.2$

Fig. 5

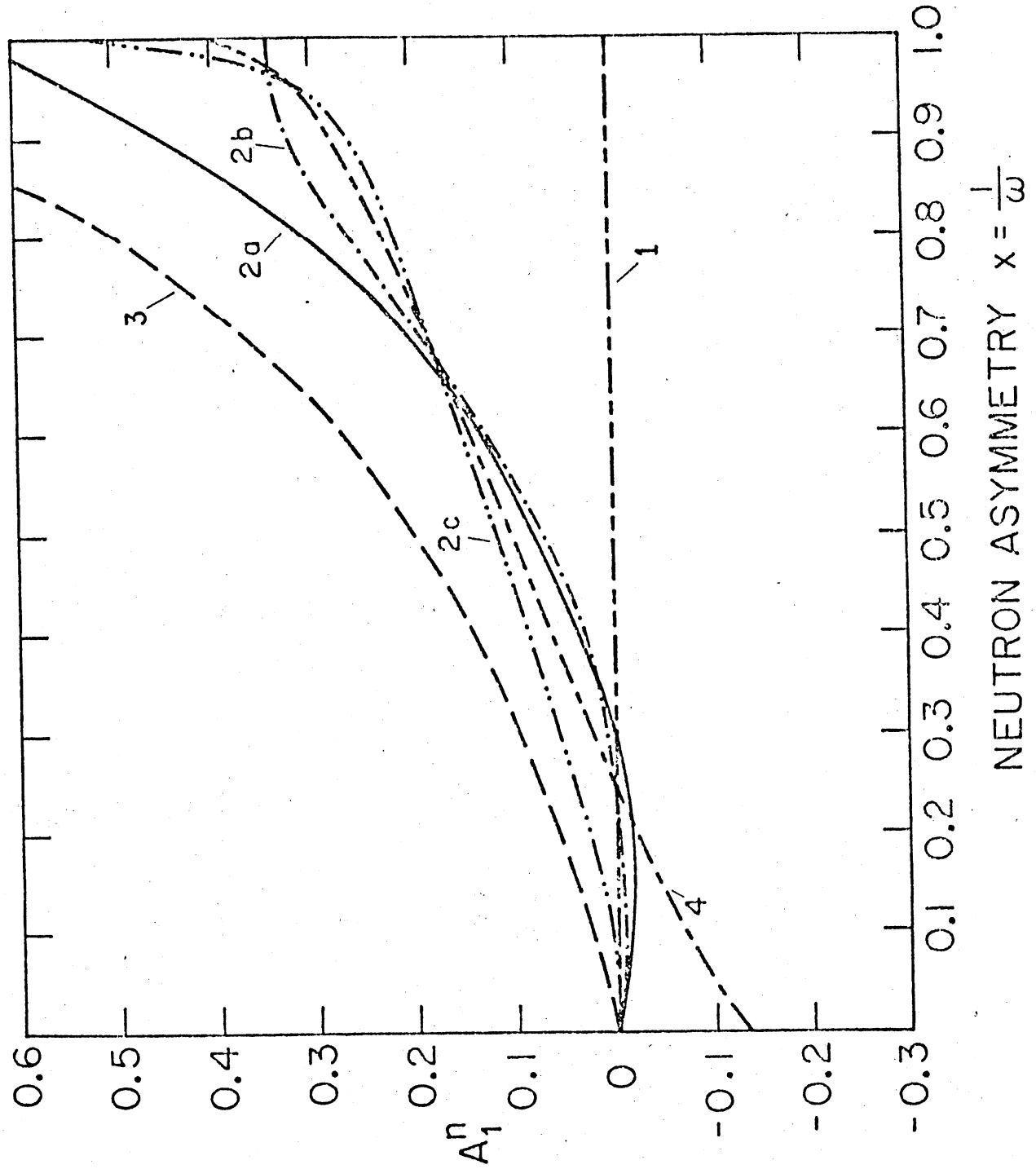
0.6
0.5
0.4
0.3
0.2
0.1
0
-0.1
-0.2
-0.3
A_1^n
0.1 0.2 0.3 0.4 0.5 0.6 0.7 0.8 0.9 1.0
NEUTRON ASYMMETRY $x = \frac{1}{\omega}$
1
2a
2b
2c
3
4

Fig. 6

1. $x \to 1$ region $(0.5 \leq x \leq 1.0)$

There are two classes of theories as seen in Fig. 5 which give

I. $A^p \to 0.6 \pm 0.05$

II. $A^p \to 1$

It will clearly be very valuable to obtain A_1^p values with higher accuracies in the range of $x = 0.5$ as proposed (Table 9). Such data could be important in the choice between these two classes of models.

2. Central region $(0.2 \leq x < 0.5)$

Experimental data are most easily obtained here. Improved accuracies with $\Delta A^p \simeq 0.03$ will be useful in establishing small differences between model predictions. Data can be obtained over a wide range of Q^2 for a test of scaling. Furthermore, it is in this region that the neutron asymmetry will be measured, and accurate proton data are required in order to determine A_1^n from asymmetry data on the deuteron.

3. $x \to 0$ region $(0 \leq x < 0.2)$

Predictions of the models are less certain and even the sign of the asymmetry is an open question. Improved data out to $\omega \sim 13$ should be very useful. Radiative corrections will be important.

Data on the neutron asymmetry A^n will be exploratory and will test the qualitative predictions of the quark-parton models. In the central region $0.1 \leq x < 0.4$ where we propose to measure A_1^n to $\sim \pm 0.05$, the models predict that A_1^n will have a small positive value.

As we point out in our Physical Review Letter (M.J. Alguard et al., Phys. Rev. Lett. 37, 1261 (1976) our experimental data on the asymmetry in the scattering of longitudinally polarized electrons by longitudinally polarized protons determines only the virtual photon proton asymmetry ($A_1^p + \eta A_2^p$). The kinematic factor η is relatively small and, taken together with the positivity limit $|A_2^p| < \sqrt{R}$, the upper limit on ηA_2^p is about equal to the statistical errors for our E80 data. Furthermore, quark-parton models predict that A_2^p will be smaller than its positivity limit. Hence we have neglected this term in comparisons of our measured asymmetry values with theoretical values for A_1^p.

With the improved precision in values of A_1^p proposed here, the above approximation may no longer be valid and it will be important to obtain experimental data on A_2^p in order to determine A_1^p alone. Although the asymmetry $A_2^p = \frac{\sigma_{TL}}{\sigma_T}$ arises from an interference between longitudinal and transverse photons and does not appear to be a crucial quantity for the theories at present, it would still be valuable to test the general qualitative theoretical prediction that A_2^p is very small.

Measurements of A_2^p can be made with transverse polarization of the proton target. We have the major items of a suitable transversely polarized proton target from experiments with a polarized target at Brookhaven. The PEGGY source and spectrometer would be applicable.

We may at a later date submit a proposal to do measurements of A_2^p, which will require about 300 hrs of data-taking time.

A major experiment is being planned and prepared for the SPS at CERN (European Muon Collaboration) to measure the asymmetry A in deep inelastic scattering of polarized muons by polarized protons. Their data will be obtained at much higher ν and Q^2 than our SLAC data; the ω range to be covered extends from $\omega \simeq 1.5$ to $\omega \simeq 20$. Their projected statistical accuracies are comparable to our SLAC E80 results and hence a factor of 3 to 4 worse than our projected E130 results. The SLAC and CERN experiments will particularly usefully complement one another in providing a test for scaling of A_1^p. It is of course always useful to study a process both with electrons and with muons and thus be able to test μe universality.

As a general conclusion we emphasize that the polarized e-p and e-n scattering experiments provide a unique type of data, which can test the general concepts of sum rules and scaling and also provide information about the spin structure of the nucleon.

European Muon Collaboration, CERN proposal July 1, 1974; Addendum September, 1976.

References

J. Kuti and V.F. Weisskopf, Phys. Rev. D 4, 3418 (1971).

R. Blankenbecler et al., SLAC-PUB-1531 (1975).
See also G.R. Farrar, Nucl. Phys. B 77, 429 (1974).

R. McElhaney and S.F. Tuan, Phys. Rev. D 8, 2267 (1973).
J.T. Dankin and G.J. Feldman, Phys. Rev. D 8, 2862 (1973);
See also G. Altarelli, N. Cabibbo, L. Maiani, and R. Petronzio, Nucl. Phys. B 69, 531 (1974). J. Okada, S. Pakvasa and S.F. Tuan, Lett. Nuovo Cimento 16, 555 (1976).
V. Barger and R.J.N. Phillips, Nucl. Phys. B 73, 269 (1974).
See also H.P. Paar and E.A. Paschos, Phys. Rev. D 10, 1502 (1974).

R. Feynman, Photon and Hadron Interactions, (W.A. Benjamin, Reading, Mass., 1972)

F.E. Close, Phys. Lett. 43B, 422 (1973).
Flume-Gorczyca and S. Kitakado, DESY Report 74/48 (1974).
G.R. Farrar and D.R. Jackson, Phys. Rev. Lett. 35, 1416 (1975).

J. Schwinger, Proc. Nat. Acad. Sci. 72, 1 (1975).

J. Schwinger, Proc. Natl. Acad. Sci. 73, 3351 (1976).

J. Schwinger, "Deep Inelastic Sum Rules in Source Theory," preprint, 1977.

E.W. Colglazier and R. Rajaraman, Phys. Rev. D 10, 334 (1974).

M.A. Ahmed and G.G. Ross, Phys. Lett. 56B, 385 (1975).

L.W. Mo, Proceedings of the 1975 Intern. Symposium on Lepton and Photon Interactions at High Energies, Stanford University, ed. W.T. Kirk (Stanford Linear Accel. Center, Stanford, Calif., 1975), p. 651;
C. Chang et al., Phys. Rev. Lett. 35, 901 (1975).

R.E. Taylor, Proceedings of the 1975 Intern. Symposium on Lepton and Photo Interactions at High Energies, Stanford University, ed. W.T. Kirk (Stanford Linear Accel. Center, Stanford, Calif., 1975), p. 679.

C.H. Lewellyn-Smith, Proceedings of the 1975 Intern. Symp. on Lepton and Photon Interactions at High Energies, Stanford University, ed. W.T. Kirk (Stanford Linear Accel. Center, Stanford, Calif., 1975), p. 709.

III. Description of Experiment

Introduction

The principles and techniques of our proposed experiment are essentially the same as for our SLAC E80 experiment. PEGGY will be used as the polarized electron source and our present polarized target, still operating at $1^{\circ}K$, will also be used. Modest modifications in PEGGY will result in an increase in beam intensity by a factor of 2. Modest changes in the target will achieve higher proton polarization, and provide polarized deuterons. The major improvement over E80 will be obtained with a new fixed-angle large-acceptance spectrometer operating at a momentum up to 18 GeV/c. It will have lower angular and momentum resolutions than the 8 GeV/c spectrometer, but the resolutions will be quite adequate for our deep inelastic studies. The spectrometer will have an acceptance 7.5 times that of the 8 GeV/c spectrometer, and at the higher operating energies more favorable kinetic points provide an additional improvement factor of 3.

The new spectrometer, together with the modest modifications in PEGGY and in the polarized target, should thus increase our effective data acquisition rate by about a factor of 40.

Polarized Electron Source

The Yale-SLAC polarized electron source, PEGGY, was continually improved (Alguard et al., 1977) throughout the duration of E80 to the point where an average intensity of 0.88×10^9 e^-/pulse at GeV energies was achieved during the last two weeks of running. In fact, during periods lasting several hours, intensities of 1.1×10^9 e^-/pulse were sustained. At the same time, the overall availability of PEGGY was increased to 75%. All of the pertinent operating characteristics of PEGGY are summarized in Table 3.

Although the performance characteristics of PEGGY were quite satisfactory for E80, several improvements in the source are possible without major modification. As a result of improved uv optical technology it will be possible to remove the uv interference filter (which rejects the 670.8 nm Li resonance radiation) and the existing aluminized MgF_2 overcoated diagonal mirror and to replace this combination with a single dielectric mirror. The reflectivity of the dielectric mirror over the relevant bandwidth (180 nm-230 nm) is estimated by Acton Research to be 0.85; virtually all 670.8 nm radiation will be rejected. This reflectivity is to be contrasted with the effective optical efficiency of 0.39 for the existing filter and mirror combination. Thus a gain of a factor of 2.2 in electron intensity can be expected. An additional gain in electron intensity of a factor of 1.2 is expected from refurbishing of the ellipsoidal mirror, giving an overall gain of 2.6.

We therefore anticipate that PEGGY will be able to provide ~2.8 x 10^9 e^-/pulse at GeV energies with no degradation in electron polarization. Since radiation damage of the target will restrict useful operation to ~1.5x10^9 e^-/pulse we expect to be able to reduce the intensity of the Li atomic beam thereby extending the lifetime of the Li oven load to >200 hrs and increasing the availability of the source to 85%, as indicated in Table 3. Should higher electron intensities be required at any time, we are modifying the oven and collimator system to produce an atomic beam with an intensity about 1.5 times greater than the existing beam. This will provide the capability of producing an electron intensity of ~4x10^9 e^-/pulse on target with a Li oven load lifetime of ~150 hrs. All the improvements require minimal modification and could be implemented by the fall of 1977. The anticipated PEGGY characteristics for E130 are summarized in Table 3.

M.J. Alguard et al., SLAC-PUB-1902, 1977, submitted to 1977 Particle Accelerator Conference, Chicago, Illinois, March 16-18, 1977.

Table 3. Operating Characteristics of Polarized Electron Beam

Characteristics	Experimental Value 12/76	Projected Value For E130
Pulse length	1.5 μs	No change
Repetition rate[a]	180 pps	No change
Electron intensity at GeV energies		
Average	0.88×10^9 e^-/pulse[b]	$>2 \times 10^9$ e/pulse
Maximum	1.1×10^9 e^-/pulse[c]	
Pulse to pulse intensity variation	<5%	<5%
Electron polarization	0.85	0.85
Polarization reversal time	3s	3s
Intensity difference upon reversal[d]	<5%	~1%
Lifetime of lithium oven load[e]	175 h	200 h
Time to reload lithium	43 h	36 h
Overall availability	75%	85%

[a]Modulator and flash lamp are usually operated at a repetition rate of 180 pps with 120 pps injected into accelerator and 60 pps used for polarization measurement at low energy.

[b]Based upon final two weeks of E80.

[c]Sustained for periods of several hours.

[d]During E95 it was shown that the intensity difference can be reduced to <1%.

[e]Based upon 740g capacity of oven.

Polarized Target

The existing Yale-SLAC polarized target can be used for the experimer without major modifications. Either normal or deuterated butanol can be polarized in the same apparatus, since both protons and deuterons interact with the electron spin reservoir in exactly the same way. (Borghir and Scheffler, 1971) For a given spin temperature T_s, deuteron polarizations are much lower than proton polarizations; a deuteron polarization of 22% corresponds to the 80% proton polarizations projected for E-130 for unirradiated target material. The only hardware addition required for deuterons is a 32 MHz DMR system for measuring the polarization.

Our main effort on the target will be devoted to improving the proton polarization to 80% and the polarizing times to 2 min, as has been achieved at other laboratories (Borghini et al., 1971; Hartman et al., 197 with 50 kG - 1°K targets albeit with smaller target volumes. Projected target operating characteristics are listed in Table 4.

The main performance limitation of our target in E80 was inadequate microwave power. Only ~5% of the generated microwave power was delivered to the target material; we hope to double this efficiency. Also, oscillators with twice the power output of our carcinotron are now commerically available. Improving the cryogenics will lower the temperature, accomodate more microwave power, and also significantly reduce the microwave power needed to achieve a given T_s. We are now setting up the target in the cryogenics building and will search for possible heat leaks, constrictions, oscillations, etc., that may be

reducing the cryostat's performance but can be eliminated once isolated. Should a further reduction in temperature be desirable, additional pumping capacity could be procured and installed without difficulty.

The deuteron polarization will be determined by techniques based on measuring the lineshape and measuring T_s through the polarization of the ~2% free protons present in the sample (Guckelsburger and Udo, 1976). In addition, the method of weighing individual targets will give an independent measurement. Both methods should be accurate to ~5%.

M. Borghini and K. Scheffler, Nucl. Instr. and Method. 95, 93 (1971).

M. Borghini, et al., Nucl. Instr. and Meth. 97, 577 (1971).

K. Guckelsberger and F. Udo, to be published.

G. Hartman, et al., Nucl. Instr. and Meth. 106, 9 (1973).

Table 4: Operating Characteristics for Polarized Target

	E-80	E-130 Proposed	CERN (Borghini et al., 19
Temperature	1.05°K	1.0°K	1.0°K
Magnetic field	50 kG	50 kG	50 kG
Cooling power	~700 mW	~700 mW	
Volume	25 cm^3	25 cm^3	0.25 cm^3
Beam heat load	~125 mW at 100 μA	~190 mW at 150 μA	
Microwave power	100-200 mW	~500 mW	~200 mW/cm
Annealing time	45 min.	30 min.	
Polarizing time			
Protons	4 min.	2 min.	
Deuterons		5 min.	5 min.
Polarization (no radiation damage)			
Protons	68%	75-80%	86±4%
Deuterons		16-22%	26±2%
Average polarization (including radiation damage)			
Protons	50%	55%	
Deuterons		12%	

Beam Energy

19.4 GeV is at present the highest one of the magic energies at which the electrons arrive at the pivot with longitudinal polarization after precessing through the 24.5° bend from the accelerator. However, with a small additional bend we can shift the magic energy. For kinematic reasons we like to run at the highest practical beam energy. Our plan is to use 22 GeV with an additional bend of 13 mrad in the beam achieved with a deflector magnet (5D36) just upstream of the polarized target (Fig. 7). The PEGGY beam can be dumped in the SEQ, as during E80. However, it should be located at the end of ESA far away from the detectors, and it should be well shielded in order to minimize background. An energy of 19.4 GeV could be a satisfactory fall back value.

New Spectrometer

Data taking for E80 has been limited by very low event rate, which was as low as 0.002 events/pulse for our most difficult point at $\omega=2$, $Q^2=4$. The polarized target can not be exposed to a much greater dose of electrons because of the radiation damage that goes along with it. Therefore a spectrometer that has a much greater acceptance than the 8 GeV spectrometer is required.

Basically the spectrometer can be simple because we do not require high momentum or angular resolution. We had originally proposed to adopt the E122 spectrometer design (Sato, 1976) which features three magnets (B201, Q82, B81) of the 8 GeV and 20 GeV spectrometers. Since we cannot take advantage of the focusing property of the quadrupole, we have studied the simpler configuration with only the two bending magnets B201 and B81 (Figs. 9,10, 11). This gives us a further gain in solid angle by a factor of 1.5 as compared to the E122 scheme while it still covers a large (50%) momentum bite. Overall we gain a factor of 7.5 in acceptance $\Delta\Omega$ $\Delta p/p$ as compared to the 8 GeV spectrometer used in E80 (Table 5).

Table 9 gives several kinematic points in the continuum that would be obtained with this spectrometer. The large momentum acceptance is well matched to the entire ω range of interest from 2.5 to 13. Thus all these data would come from one spectrometer setting ($\theta=5^\circ$), and indeed fluctuations in target polarization, for example, would have no effect on the ω dependence. Table 8 covers the low ω, high Q^2 range that would be obtained with a $\theta = 10^\circ$ setting.

T. Sato, "The Spectrometer for E122," 8/3/76, Group A Engineering Note 66.

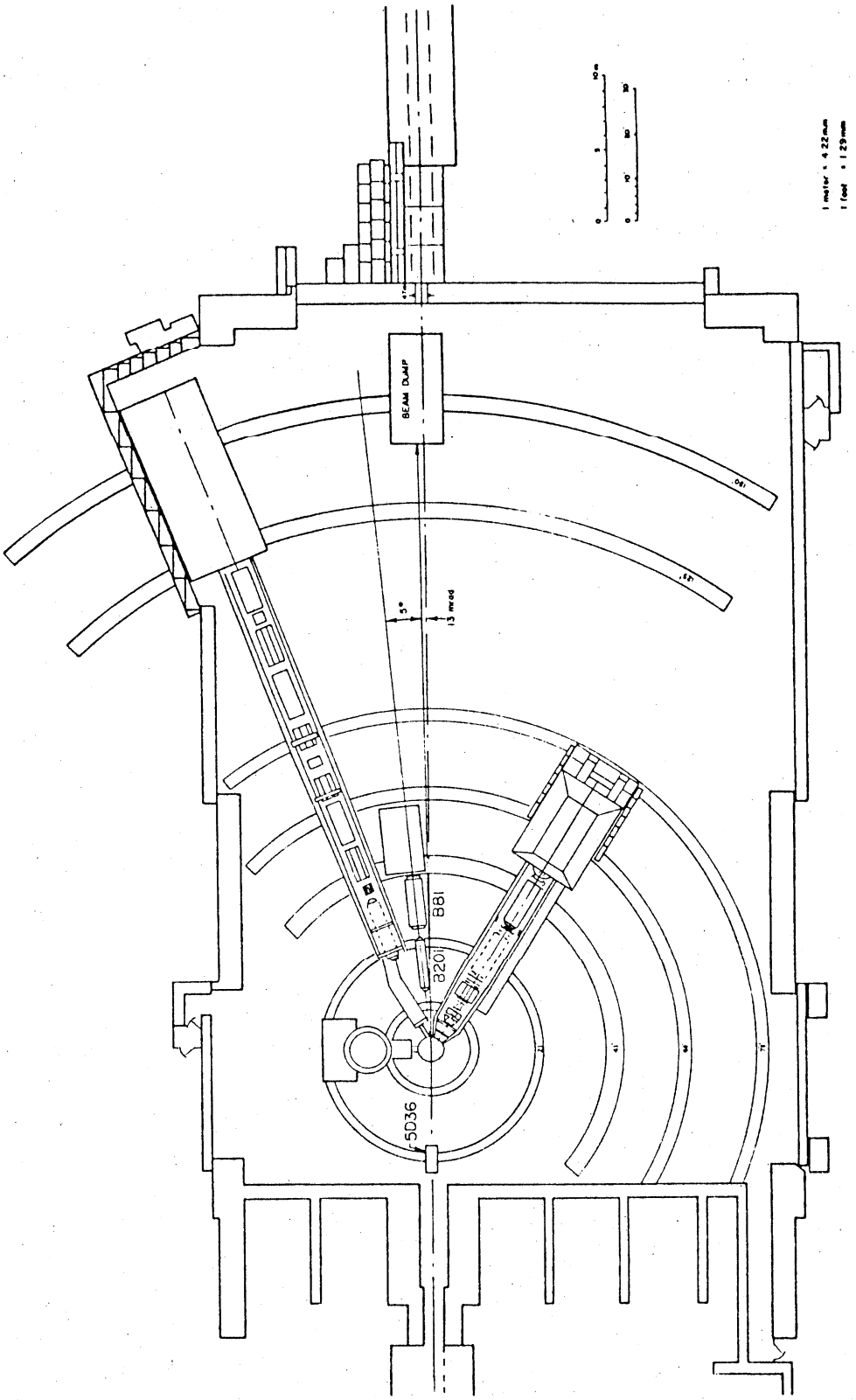

Fig. 7

Table 5: Spectrometer

	E130 Spectrometer	8 GeV spectrometer (for comparison)
$\Delta p/p$	±25%	±2%
$\Delta\theta$	±7.5 mrad	±7 mrad
$\Delta\phi$	±15 mrad	±27 mrad
$\Delta\Omega$	0.45 msr	0.75 msr
$\int\Delta\Omega\,\Delta p/p$	0.22 msr	0.03 msr

Fig. 8 shows a layout of the spectrometer. The scattering angle ϑ is recorded in the horizontal plane. Momentum dispersion is in the vertical plane, orthogonal to ϑ. The bending angle of $2x7^{\circ}$ is sufficient to block the straight line of sight between target and detector Yet the required excitation of the magnets at 15 GeV/c is modest and the field inhomogeneities are less than 1% across the used gapwidth. The trajectories are recorded in four planes of proportional wire chambers (PWC) and determine momentum and scattering angle to an accuracy of $\Delta p/p = \pm 1\%$ and $\Delta\vartheta = \pm 0.1$ mrad. At our kinematic settings (Table 8 to 10) this translates into resolutions for ω and Q^2 of $\Delta\omega/\omega \approx \pm$ (2 to 5)% and $\Delta Q^2/Q^2 \approx \pm 1\%$, which is adequate.

Electrons are identified with a preradiator (P) - shower counter (S) combination with an expected pion rejection of at least 50 to 1. Pion contamination essentially originates from pion photoproduction and becomes worrysome only at the lower momentum bins where the π^-/e^- ratio can exceed 1. We have estimated the π^-/e^- ratios for E130 on the basis of data from SLAC experiment E89 (Table 6). In order to improve the pion rejection further we plan the addition of a long N_2-Cerenkov counter (C) operated at 0.25 atm with a pion threshold of about 12 GeV/c. Even a few GeV/c above threshold such a counter still maintains useful discriminatory power. A Cerenkov counter with an even higher threshold would become either too long or drop below 99% efficiency. Finally, there are two aperture defining counters (F,R). With the exception of the PWC's the detector arrangement is very similar to the situation in E80 (Table 7).

The multiwire proportional chambers are to be constructed with 2 mm wire spacing and are of conventional design. We are planning to have a prototype ready by August 1977.

Our group has built and owns readout electronics for 20 chamber planes which is being used in the E-61 polarization experiment at Fermilab. This readout uses serial (Dhawan,1974) transmission using one coa cable to transfer datawords between a chamber plane and a CAMAC module. This system is very flexible and adaptable to use in ESA.

The mechanical construction of the spectrometer requires that a massive fixed angle support frame be built for the two magnets and the detector housing. Helium bags rather than vacuum chambers will be used with the magnets. A detector house has to be assembled from concrete blocks. Moving from the 5° to the 10° setting will require dissassembly and reassembly of the spectrometer components. Substantial experience with regard to the cost and labor aspect of the spectrometer setup should be gained from SLAC experiment E122 which requires quite similar operations.

S. Dhawan, "A Fast readout and Geometrical Reconstruction System for Proportional Wire Chambers," IEEE Transactions on Nuclear Science, Vol. NS-21, No. 1, 1974.

Table 6: Estimated π^-/e^- ratio

p (GeV/c)	$\theta=5^o$ π^-/e^-	$\theta=10^o$ π^-/e^-
10	<6	<1.6
11	3	<1.0
12	1.5	<1.0
13	0.6	<1.0
14	0.3	<1.0
>15	<0.1	<1.0

Table 7: Detectors and Related Hardware

Qty.	Type	Proposed Deliverer
1	Lead glass shower counter (36×100 cm^2) with four phototubes (existing)	SLAC
1	Preradiator: already used in E80 with phototubes (existing)	SLAC
1	N_2-Cerenkov counter: $0.5 \times 0.9 \times 4.5$ m^3, to be operated at ~0.25 atm.	Yale
1	Cerenkov N_2 gas supply, pump and pressure controls (existing)	SLAC
2	Front and rear trigger counters	Yale
10	Proportional wire chambers: four X, four Y and two tilted chambers (35 x 85 cm each, 2 mm wire spacing); amplifiers; readout electronics and computer interface for ca. 3000 channels; magic gas supply. The readout electronics is already existing.	Yale

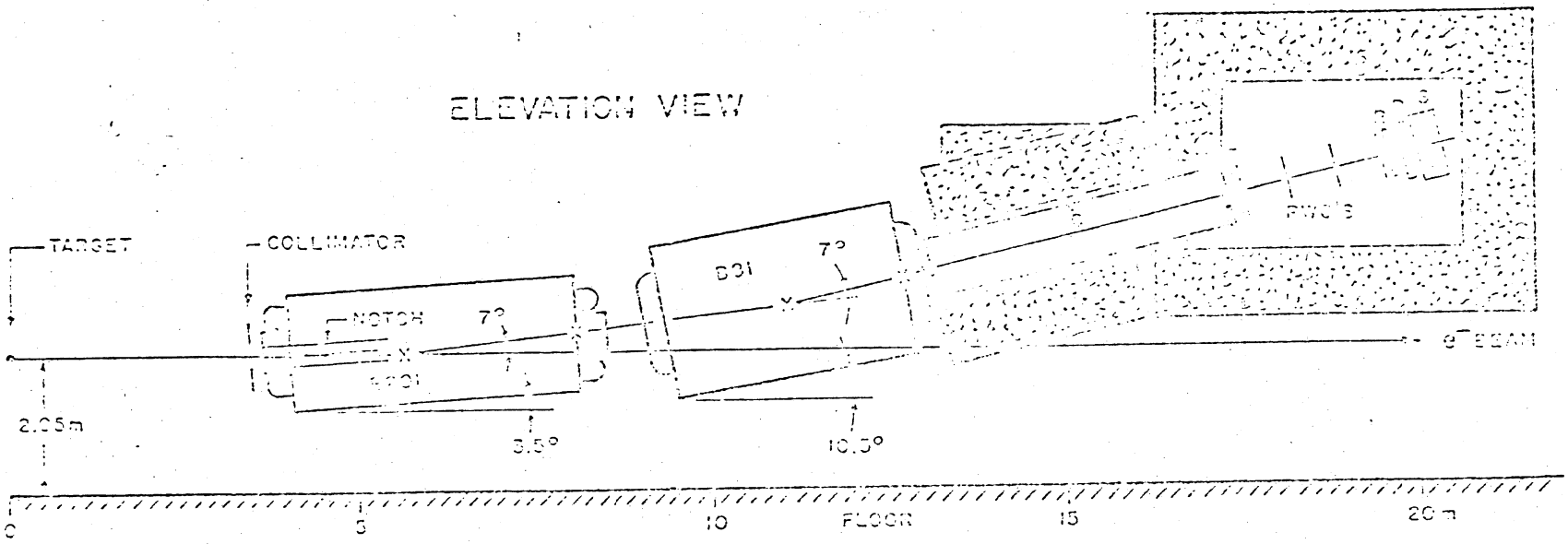

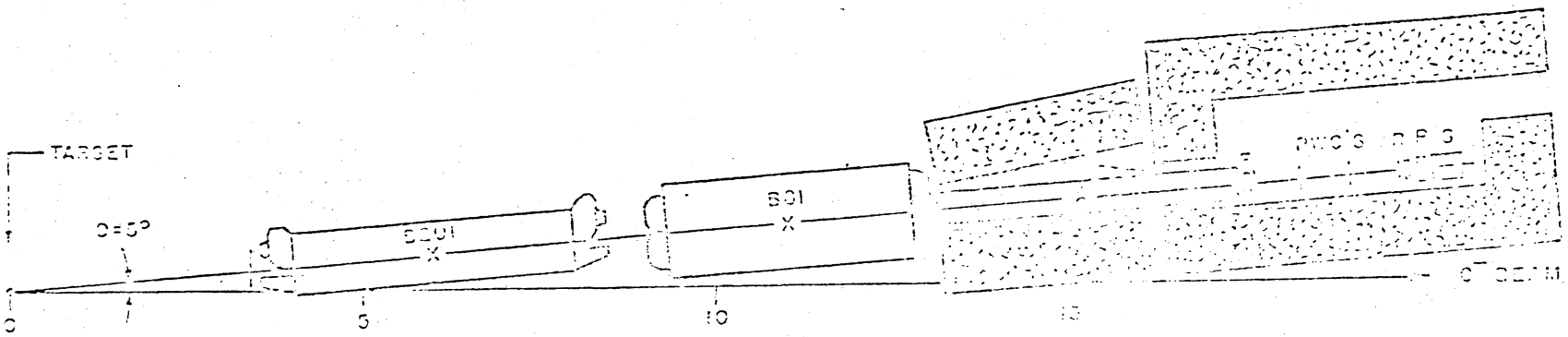

PLAN VIEW

Fig. 8

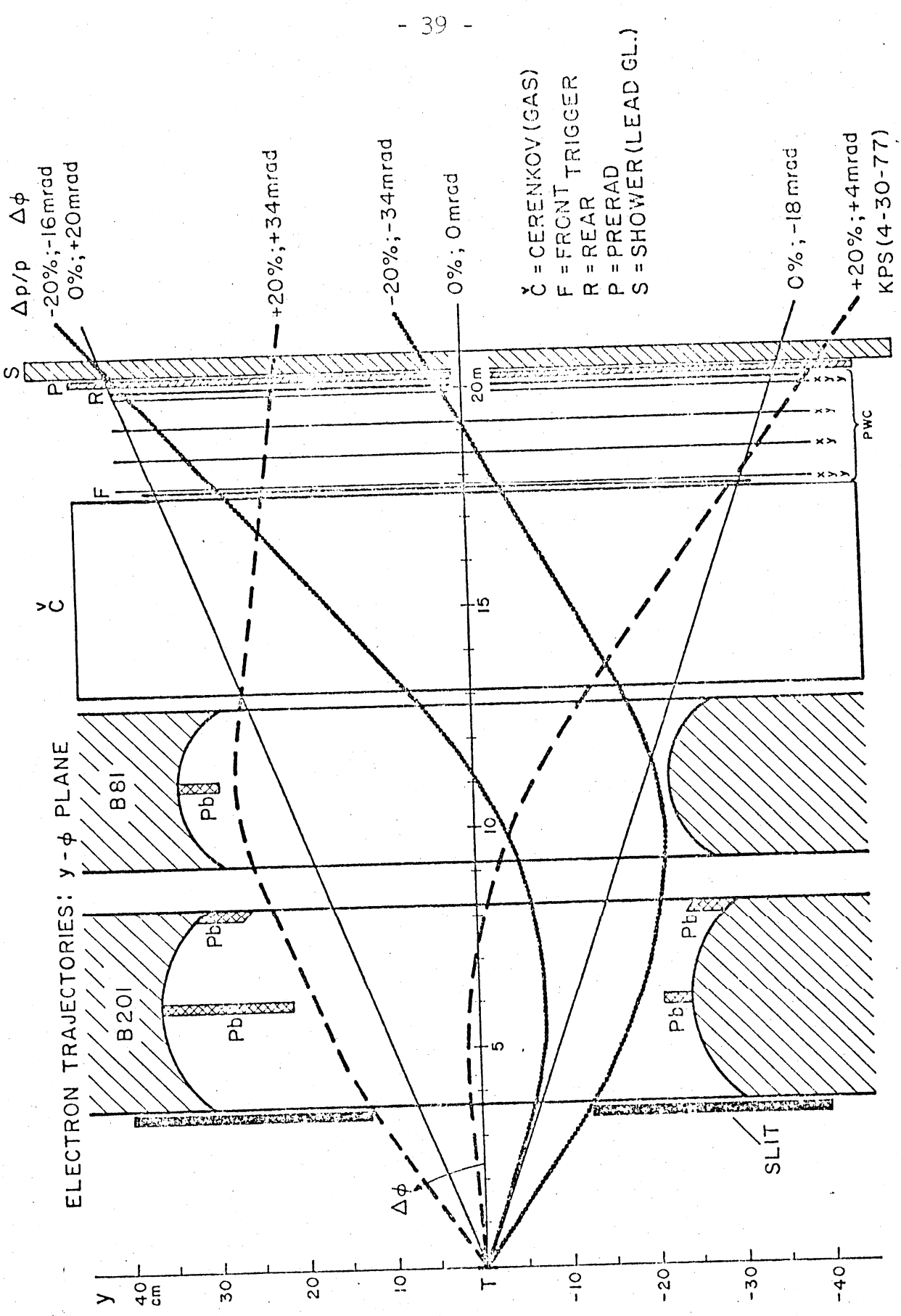
ELECTRON TRAJECTORIES: y-φ PLANE
Δp/p Δφ
-20%;-16mrad
0%;+20mrad
+20%;+34mrad
-20%;-34mrad
0%; 0mrad
0%;-18mrad
+20%;+4mrad
KPS(4-30-77)
Č = CERENKOV (GAS)
F = FRONT TRIGGER
R = REAR
P = PRERAD
S = SHOWER (LEAD GL.)
S
P
R
F
Č
PWC
20 m
B81
B201
Pb
SLIT
Δφ
y
40 cm
30
20
10
T
-10
-20
-30
-40
15
10
5

Fig. 9

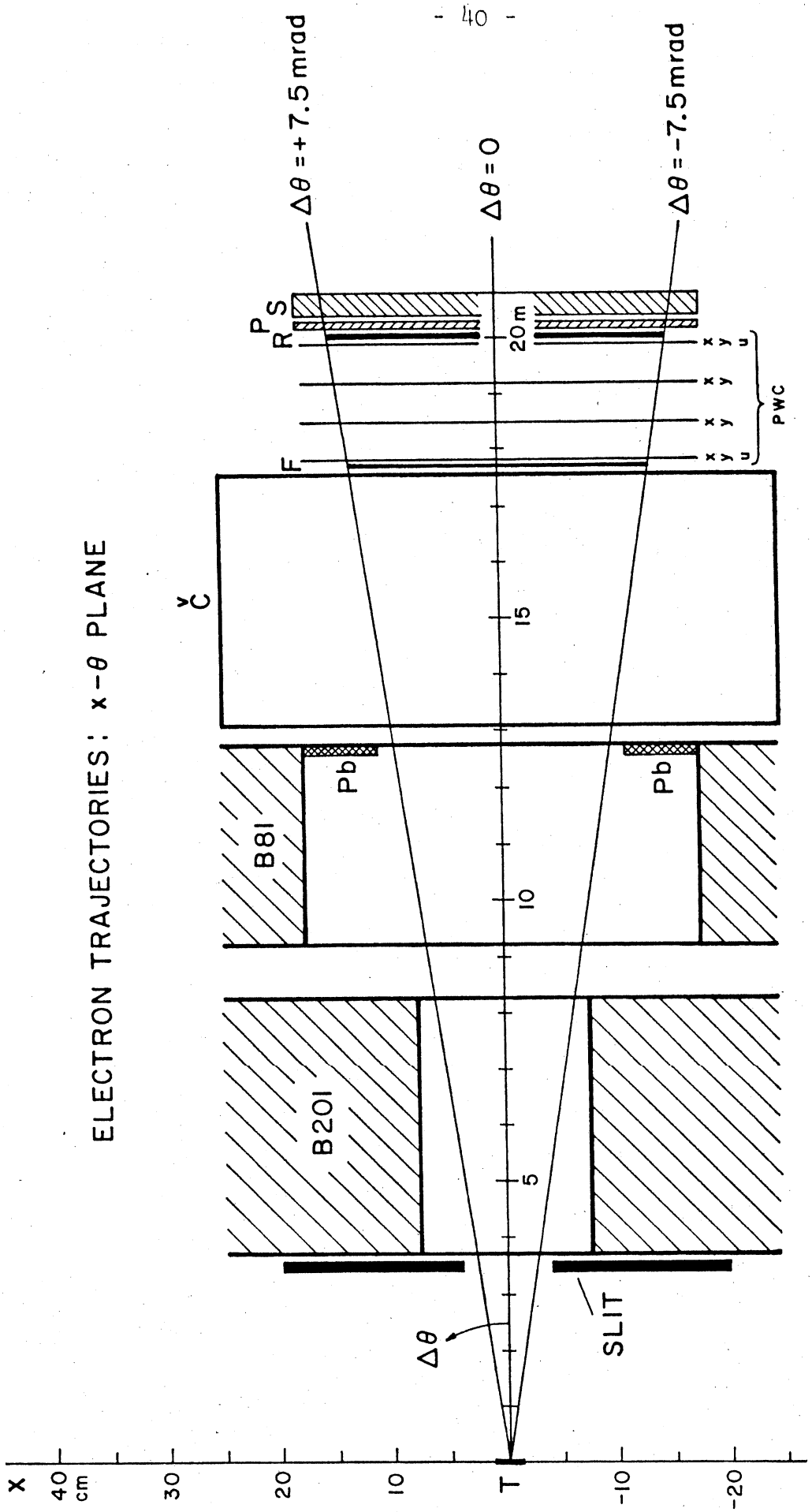
ELECTRON TRAJECTORIES: x-θ PLANE
Δθ = +7.5 mrad
Δθ = 0
Δθ = -7.5 mrad
PS
R
F
20 m
x x y u
x x y
x x y
x y u
PWC
C
B81
Pb
Pb
B201
SLIT
Δθ
X
40 cm
30
20
10
T
-10
-20
15
10
5

Fig. 10

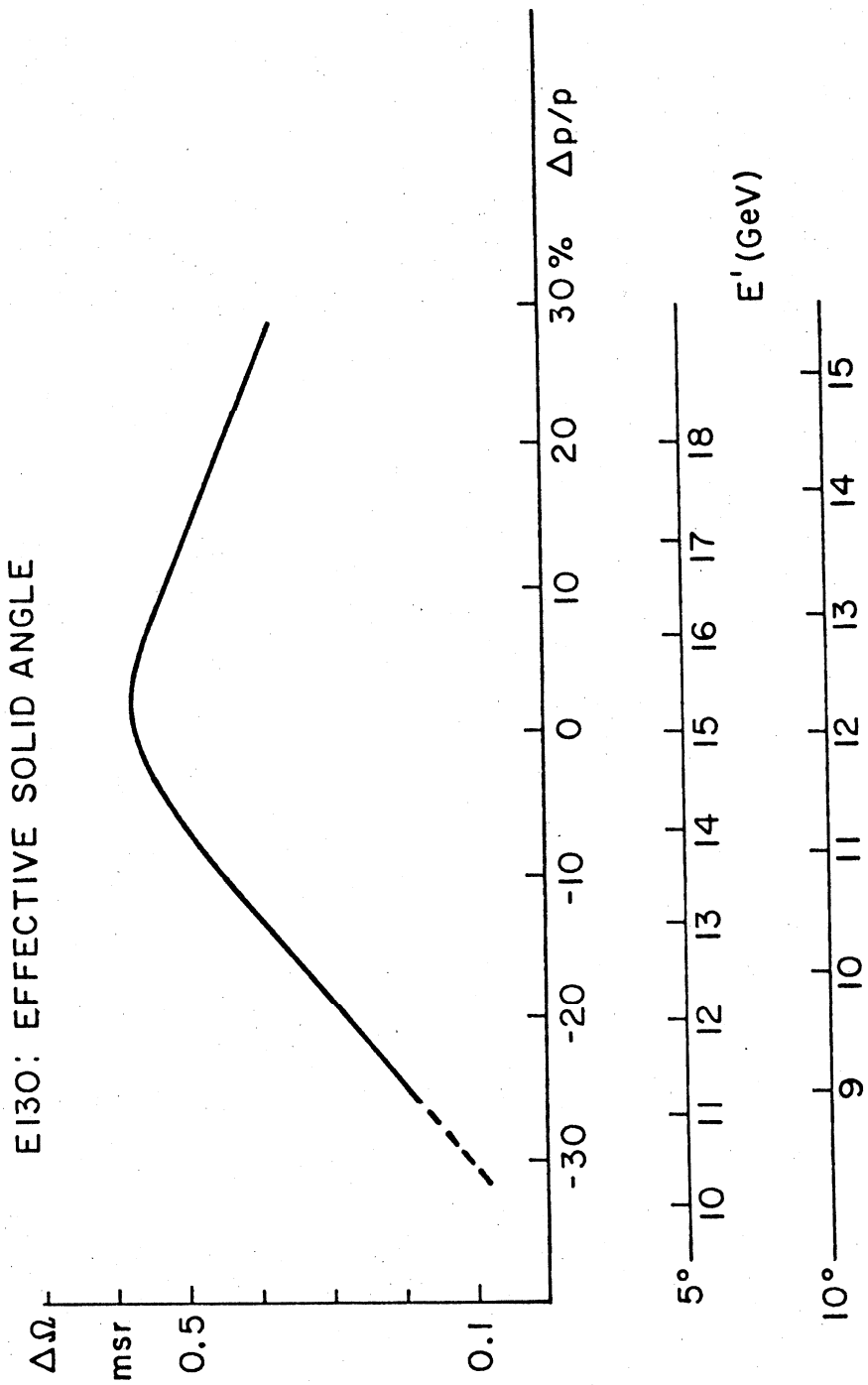
E130: EFFECTIVE SOLID ANGLE
ΔΩ
msr
0.5
0.1
-30
-20
-10
0
10
20
30%
Δp/p
E'(GeV)
5°
10°
10
11
12
13
14
15
16
17
18
9
10
11
12
13
14
15

Fig. 11

Data to be Obtained

We propose to obtain data for two settings of the spectrometer, first with $\theta = 10^{\circ}$ and second $\theta = 5^{\circ}$. The predictions for the data to be obtained are given in Tables 8, 9, and 10. Only the statistical errors are given in the Tables.

With regard to systematic errors we plan to determine the beam polarization P_e to about ±5% by Möller scattering. The proton and deuteron polarizations will be determined to about ±5% as well. Finally the fraction F will also be determined to about ±5%. These systematic errors amount to about 10% and occur as a multiplicative scale factor uncertainty.

The running time required is indicated in Table 11. We propose to measure first the proton asymmetries for $\theta = 10^{\circ}$ in one cycle of machine operation. In a subsequent cycle we will measure the proton and deuteron asymmetries for $\theta = 5^{\circ}$.

TABLE 8: Kinematics for Proton Low ω and High Q^2

E = 22 GeV

$\theta = 10^{o}$

E' GeV	ν GeV	Q^2 $(GeV/c)^2$	W GeV	ω	D	$\frac{d^2\sigma}{d\Omega dE'/E'}$ $(10^{-30} cm^2/Sr)$	M[a]	$\frac{events}{pulse}$ $x10^{-3}$ [b]	$\frac{events}{300\ hrs}$ $x10^{6}$	Error in Δ $(x10^{-2})$ [c]	Error in A_1^p [d]
15	7	10	2.0	1.3	.32	.010	.02	0.9	0.17	0.24	0.14
14	8	9.4	2.6	1.6	.37	.024	.06	2.2	0.43	0.15	0.08
13	9	8.7	3.0	1.9	.42	.040	.13	3.7	0.72	0.12	0.05
12	10	8.0	3.4	2.3	.48	.052	.20	4.5	0.87	0.11	0.05
11	11	7.4	3.8	2.8	.53	.058	.29	3.9	0.76	0.11	0.04
10	12	6.7	4.1	3.4	.58	.059	.36	2.8	0.55	0.13	0.05
9	13	6.0	4.4	4.1	.64	.058	.43				

(a) M is the figure of merit $D^2\ d^2\sigma/d\Omega dE'/E'$, which is inversely proportional to running time for a given error in A_1^p. For the ω=3, Q^2=2.7 $(GeV/c)^2$ point of E80, we take M=1.

(b) Assumes $1.5x10^9$ e^-/pulse, a 3.8 cm target of density 0.7 g/cm^3 and a 20% loss due to beam rastering.

(c) $\Delta = P_e P_p F\ A^p$ is the raw counting rate asymmetry.

(d) Assumes $A_1^p = A^p/D = \Delta/(P_e P_p F D)$ with P_e=0.85, P_p=0.55, F=0.1, and ηA_2^p=0.

TABLE 9: Kinematics for Precision Proton Data

E = 22 GeV

$\theta = 5.0^{o}$

E' (GeV)	ν (GeV)	Q^2 $(GeV/c)^2$	W GeV	ω	D	$\frac{d^2\sigma}{d\Omega dE'/E'}$ $(x10^{-30}cm^2)$	M	$\frac{events}{pulse}$	$\frac{events}{100\ hrs}$ $(x10^6)$	Error in Δ $(x10^{-4})$	Error in A_1^p
18	4	3.0	2.3	2.5	0.17	3.3	1.7	0.15	9.7	3.2	0.035
17	5	2.9	2.7	3.3	0.22	3.2	2.7	0.17	11.0	3.0	0.026
16	6	2.7	3.1	4.2	0.27	2.8	3.6	0.17	11.0	3.0	0.021
15	7	2.5	3.4	5.2	0.32	2.4	4.2	0.15	9.7	3.2	0.020
14	8	2.3	3.7	6.4	0.37	2.0	4.9	0.12	7.8	3.6	0.020
13	9	2.2	4.0	7.8	0.41	1.7	5.5	0.07	4.5	4.7	0.023
12	10	2.0	4.2	9.3	0.47	1.4	5.8	0.04	2.6	6.2	0.026
11	11	1.8	4.4	11.2	0.53	1.2	6.3	0.02	1.3	8.8	0.035
10	12	1.7	4.7	13.4	0.58	1.1	6.6				

TABLE 10: Kinematics for Deuterons

E = 22 GeV

$\theta = 5.0^{\circ}$

E' (GeV)	ν (GeV)	Q^2 $(GeV/c)^2$	W GeV	ω	D	$\frac{d^2\sigma}{d\Omega dE'/E'}$ $x10^{-30}cm^2/sr$	M[b]	events/pulse	events/200 hrs $(x10^6)$	Error in Δ $(x10^{-4})$	Error in A_1^d[a]	Error in A_1^n
18	4	3.0	2.3	2.5	.17	2.7	0.6					
								0.28	36	1.7	0.038	0.10
16	6	2.7	3.1	4.2	.27	2.5	2.1					
								0.29	37	1.6	0.025	0.06
14	8	2.3	3.7	6.4	.37	1.9	3.5					
								0.18	26	2.0	0.024	0.05
12	10	2.0	4.2	9.3	.47	1.4	4.6					
								0.06	8	3.6	0.035	0.08
10	12	1.7	4.7	13.4	.58	1.0	5.6					

a Assume $P_e P_D F = 0.02$ [P_e=0.85, P_D=0.12, F=0.2].

b A factor of $(1-1/\omega)^2$ is included to account for the smaller neutron cross section.

Table 11. Running Time

Data Collection	Factored Hours
Proton (10°) (Table 8)	300
Proton (5°) (Table 9)	100
Deuteron (5°) (Table 10)	200
	600

Check out, background, and Möller measurement

250 hrs at 10 to 30 pps

Our plan of data-taking is to obtain the $\theta = 10^{\circ}$ data in one cycle and the $\theta = 5^{\circ}$ data in a subsequent cycle.

Group Proposing Experiment

Yale

V.W. Hughes	Professor
M.S. Lubell	Associate Professor
M.E. Zeller	Associate Professor
P.A. Souder	Assistant Professor
M.J. Alguard	Research Associate and Lecturer
J.E. Clendenin	Research Associate
K.P. Schüler	Research Associate
T. Sasao	Research Staff Physicist
M.R. Bergstrom	Graduate Student
R.F. Oppenheim	Graduate Student
D.A. Palmer	Graduate Student
G. Dhawan	Electronics Engineer
R. Fong-Tom	Microwave Engineer

SLAC

R.H. Miller

S.J. St Lorant

University of Bielefeld, Germany

W. Raith	Professor
G. Baum	

University of Tsukuba and KEK, Japan

K. Kondo	Professor
S. Miyashita	
K. Morimoto	